NUCLEON STRUCTURE IN LIGHT MUONIC ATOMS

Franziska Hagelstein (JGU Mainz & PSI Villigen)

in collaboration with

V. Biloshytskyi, T. Esser, V. Lensky, V. Pascalutsa, S. Pitelis (JGU)

and V. Sharkovska (PSI, UZH)

PROTON RADIUS

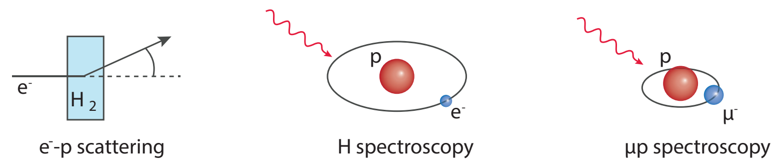

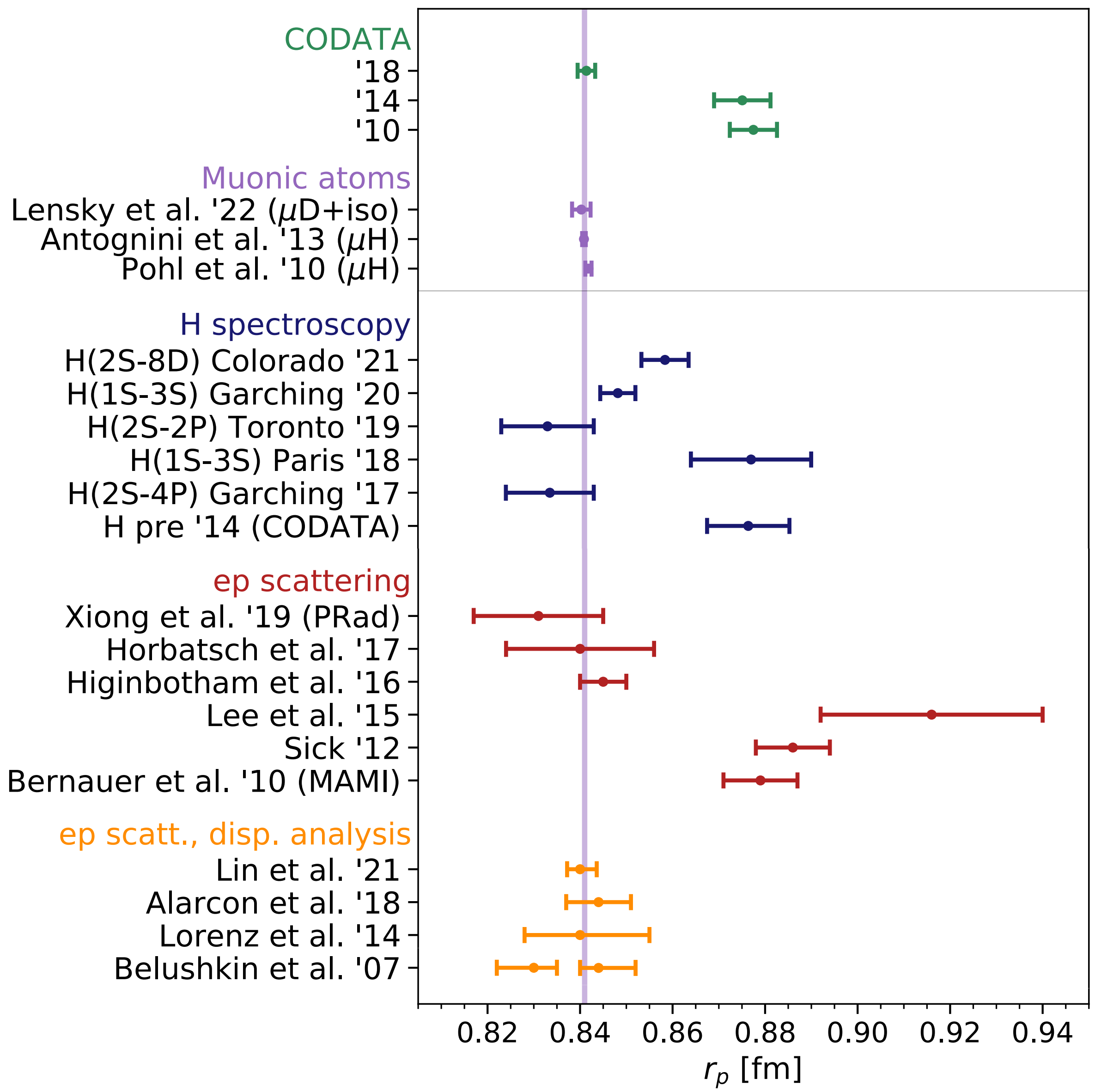

- Muonic atoms allow for PRECISE extractions of nuclear charge and Zemach radii
- CODATA since 2018 included the μH result for r_p
- Still open issues: H(2S-8D), H(1S-3S) @ Paris
- Question: PRECISION VS ACCURACY

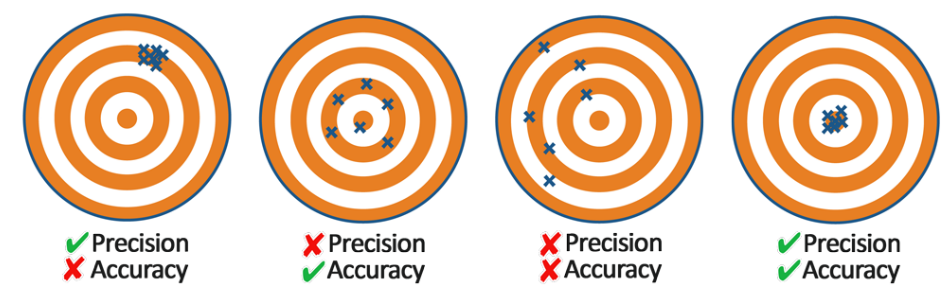

H.-W. Hammer, Wed.

PROTON RADIUS

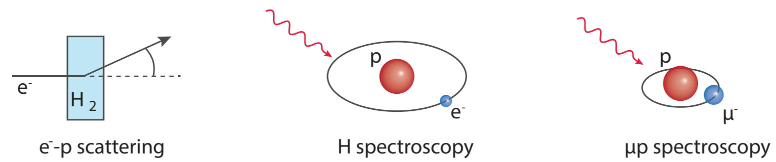

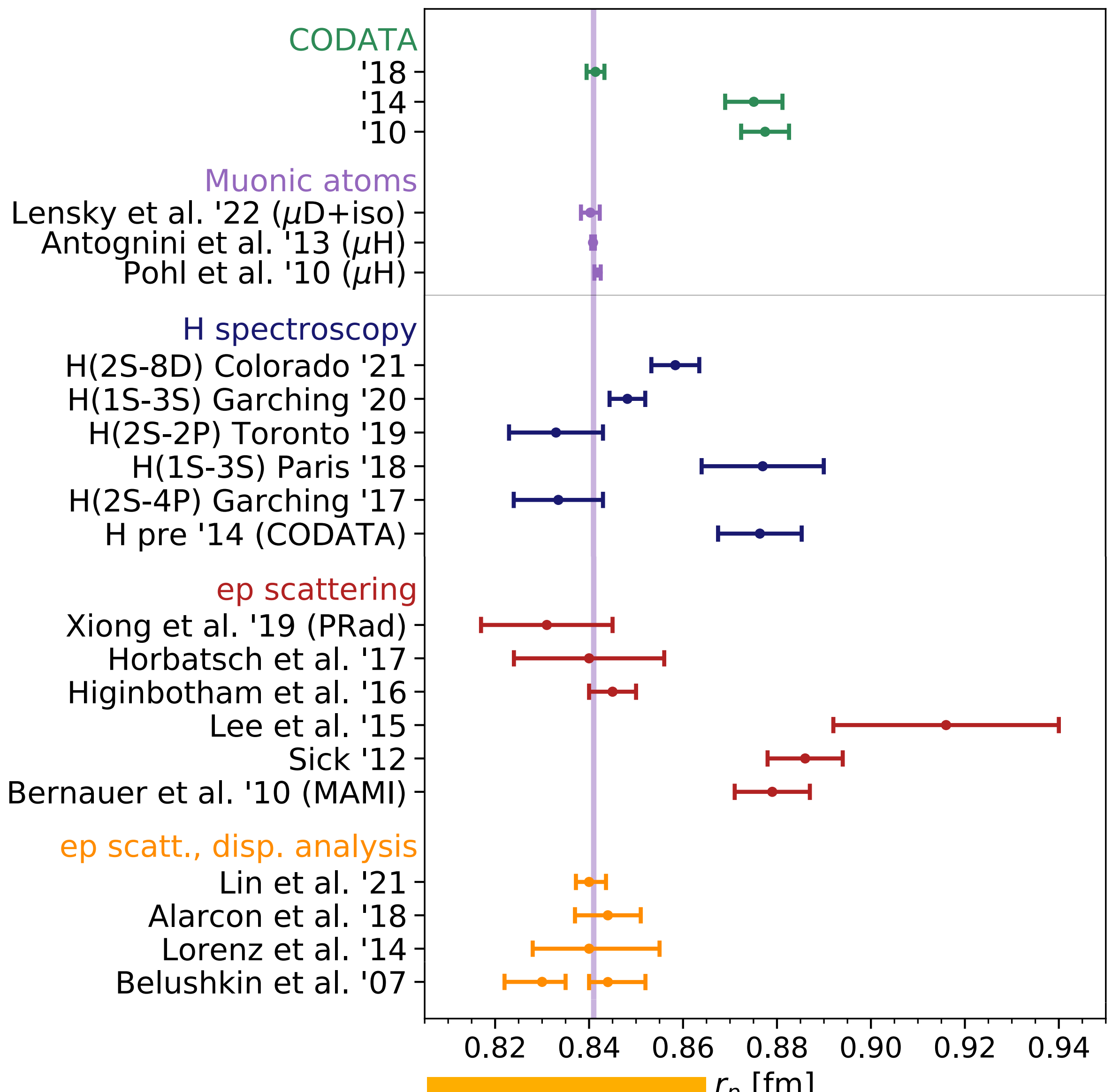

H(2S-6P) Maisenbacher @PSAS

- Muonic atoms allow for PRECISE extractions of nuclear charge and Zemach radii
- CODATA since 2018 included the μH result for r_p
- Still open issues: H(2S-8D), H(1S-3S) @ Paris
- Question: PRECISION VS ACCURACY

PRECISION ATOMIC SPECTROSCOPY

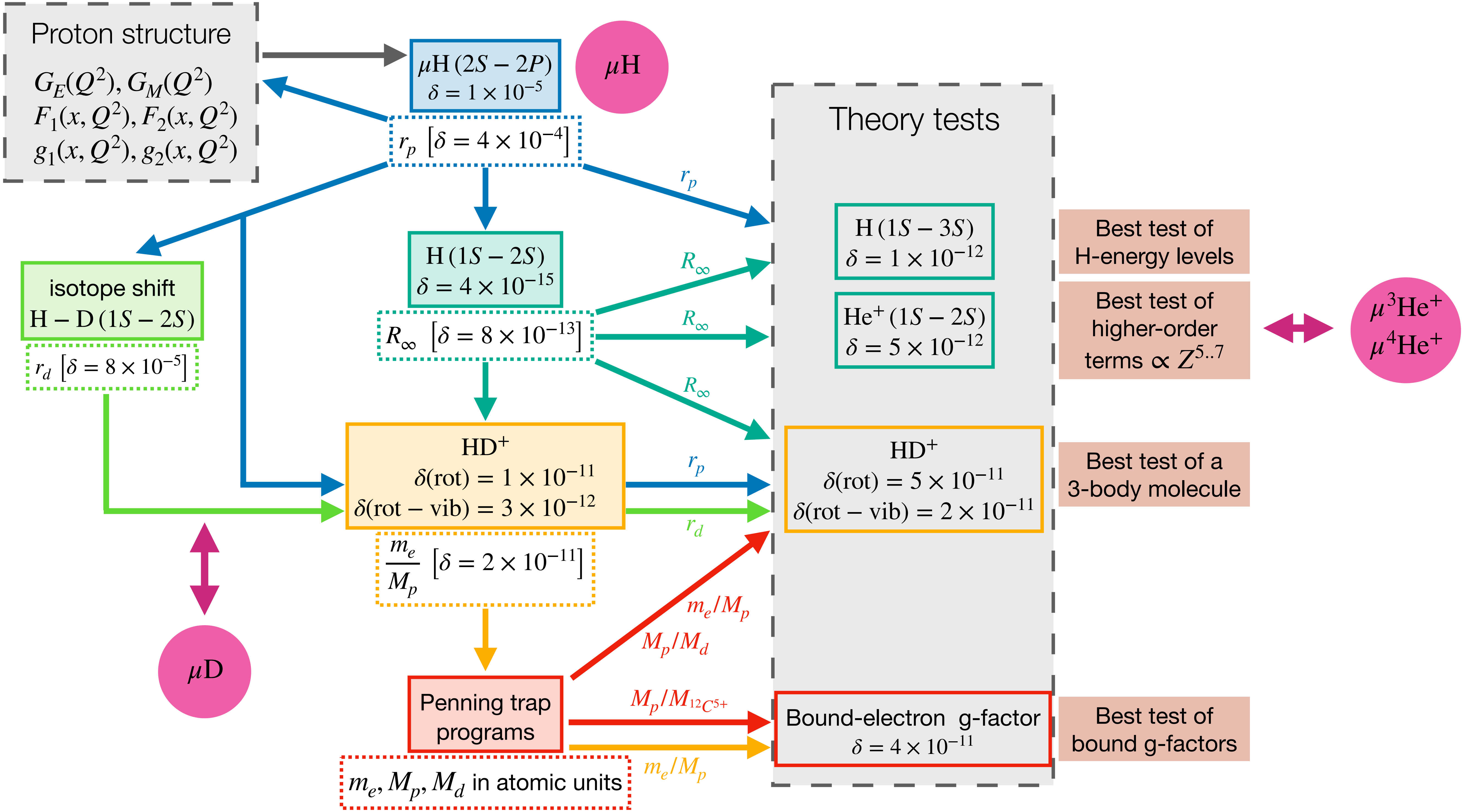

A. Antognini, FH, V. Pascalutsa, Ann. Rev. Nucl. Part. **72** (2022) 389

FROM PUZZLE TO PRECISION

- Several experimental activities ongoing and proposed:
  - 1S hyperfine splitting in μH (ppm accuracy) and μHe
  - Improved measurement of Lamb shift in μH, μD and μHe^+ possible ($\times 5$)
  - Medium- and high-Z muonic atoms

- **Theory Initiative** is needed!

Muonic Atom Spectroscopy Theory Initiative

- Initial objectives:
  - Accurate theory predictions for light muonic atoms to test fundamental interactions by comparing to electronic atoms
  - Community consensus on SM predictions
  - First emphasis on the hyperfine splitting in μH


"PREN & μASTI" workshop @ JGU, 06/23

from **PUZZLE**

ASTI

to **PRECISION**

https://asti.uni-mainz.de

"New perspectives in the charge radii determination of light nuclei"
ECT* Trento, 28.07.25 — 01.08.25

NUCLEAR STRUCTURE EFFECTS

Why muonic atoms ?

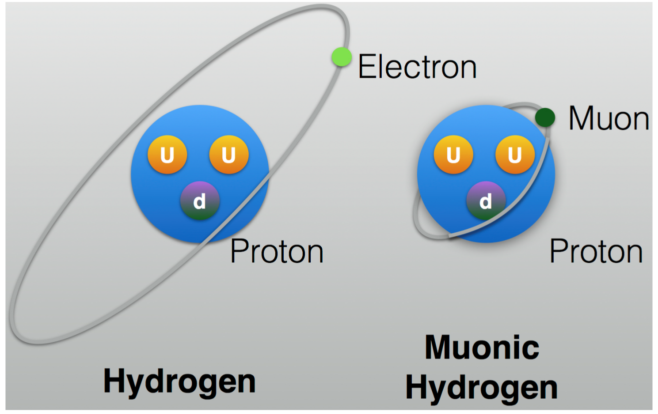

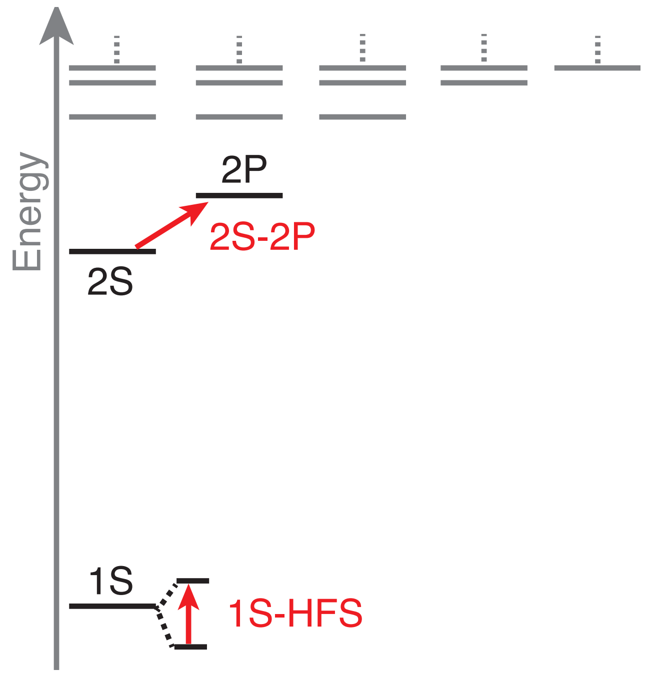

NUCLEAR STRUCTURE EFFECTS

Why muonic atoms ?

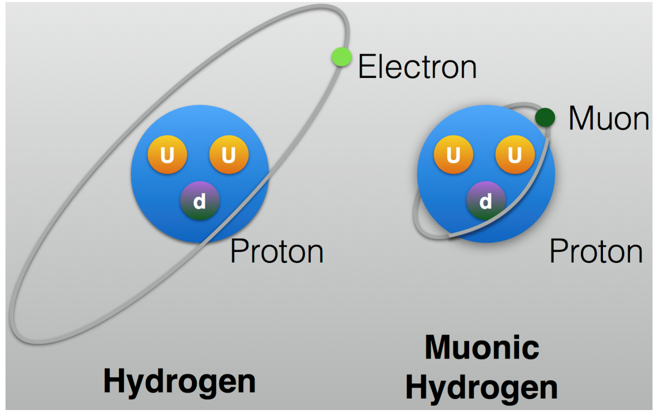

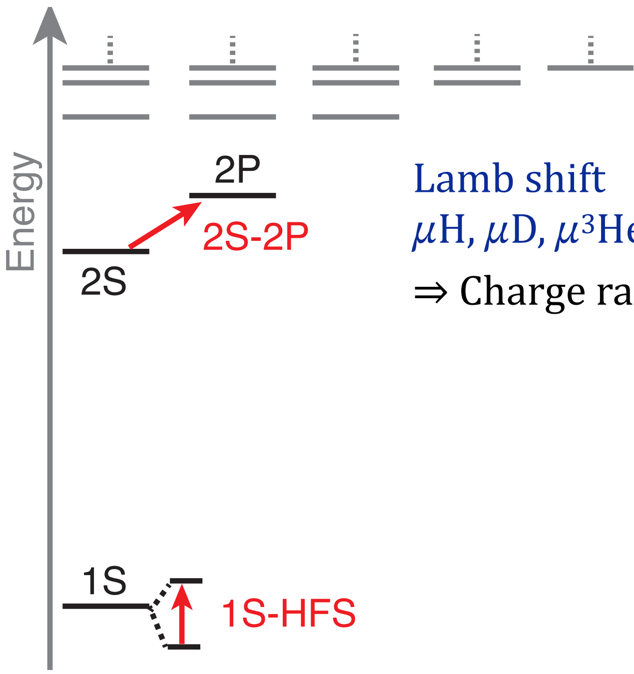

Lamb shift
μH, μD, μ^3He$^+$, μ^4He$^+$
⇒ Charge radii

- **Lamb shift:**

wave function at the origin

charge radius

Friar radius or 3rd Zemach moment

$$\Delta E_{nl}(\mathrm{LO+NLO}) = \delta_{l0}\,\frac{2\pi Z\alpha}{3}\,\frac{1}{\pi(an)^3}\left[R_E^2 - \frac{Z\alpha m_r}{2} R^3_{E(2)}\right]$$

NUCLEAR STRUCTURE EFFECTS

Why muonic atoms ?

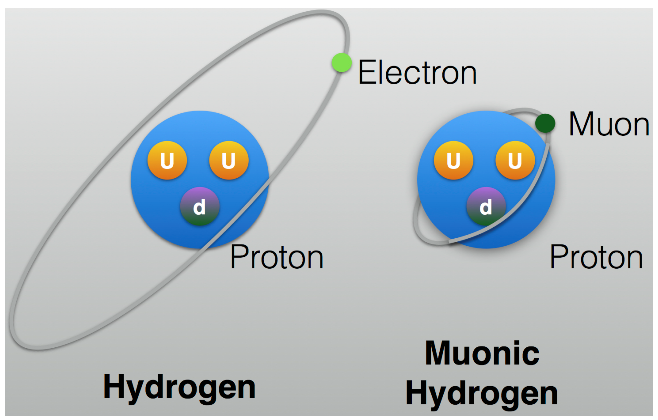

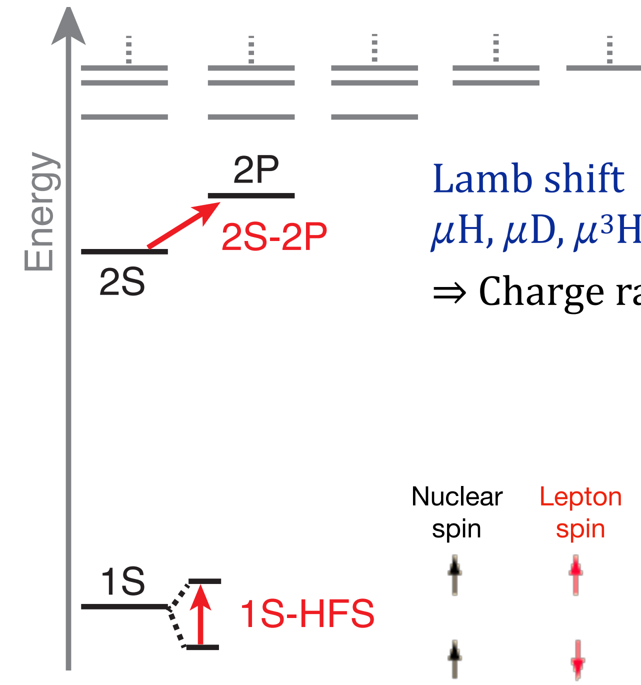

Lamb shift
μH, μD, μ^3He$^+$, μ^4He$^+$
⇒ Charge radii

Hyperfine splitting (HFS)
μH, μ^3He$^+$
⇒ Zemach radii, magnetic properties

- Lamb shift:

wave function at the origin

charge radius

Friar radius or 3rd Zemach moment

$$\Delta E_{nl}(\mathrm{LO+NLO}) = \delta_{l0}\,\frac{2\pi Z\alpha}{3}\,\frac{1}{\pi(an)^3}\left[R_E^2 - \frac{Z\alpha m_r}{2} R^3_{E(2)}\right]$$

- HFS:

Zemach radius

$$\Delta E_{nS}(\mathrm{LO+NLO}) = E_F(nS)\,[1 - 2\,Z\alpha m_r\,R_Z]$$

NUCLEAR STRUCTURE EFFECTS

Why muonic atoms ?

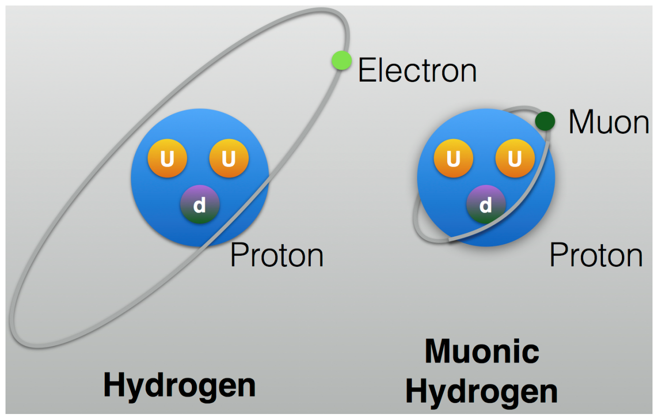

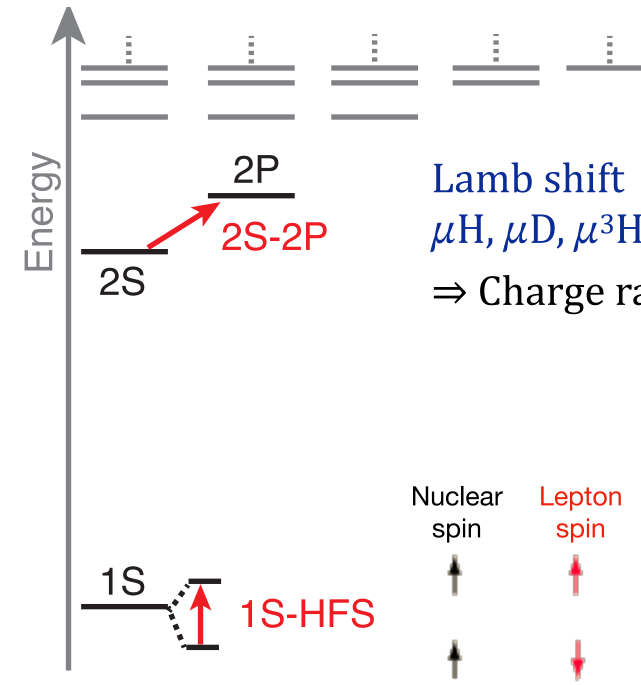

Lamb shift
$\mu H, \mu D, \mu^3He^+, \mu^4He^+$
⇒ Charge radii

Hyperfine splitting (HFS)
$\mu H, \mu^3He^+$
⇒ Zemach radii, magnetic properties

- **Lamb shift:**

wave function at the origin

charge radius

Friar radius or 3rd Zemach moment

$$\Delta E_{nl}(\mathrm{LO{+}NLO}) = \delta_{l0}\,\frac{2\pi Z\alpha}{3}\,\frac{1}{\pi(an)^3}\left[R_E^2 - \frac{Z\alpha m_r}{2}R^3_{E(2)}\right]$$

NLO becomes appreciable in μH

- **HFS:**

Zemach radius

$$\Delta E_{nS}(\mathrm{LO}+\mathrm{NLO}) = E_F(nS)\,[1-2\,Z\alpha m_r\,R_Z]$$

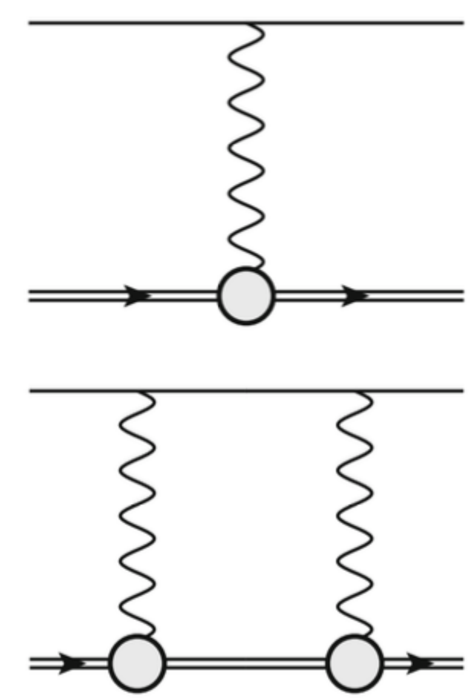

NORMAL VS. MUONIC ATOMS

muonic hydrogen:

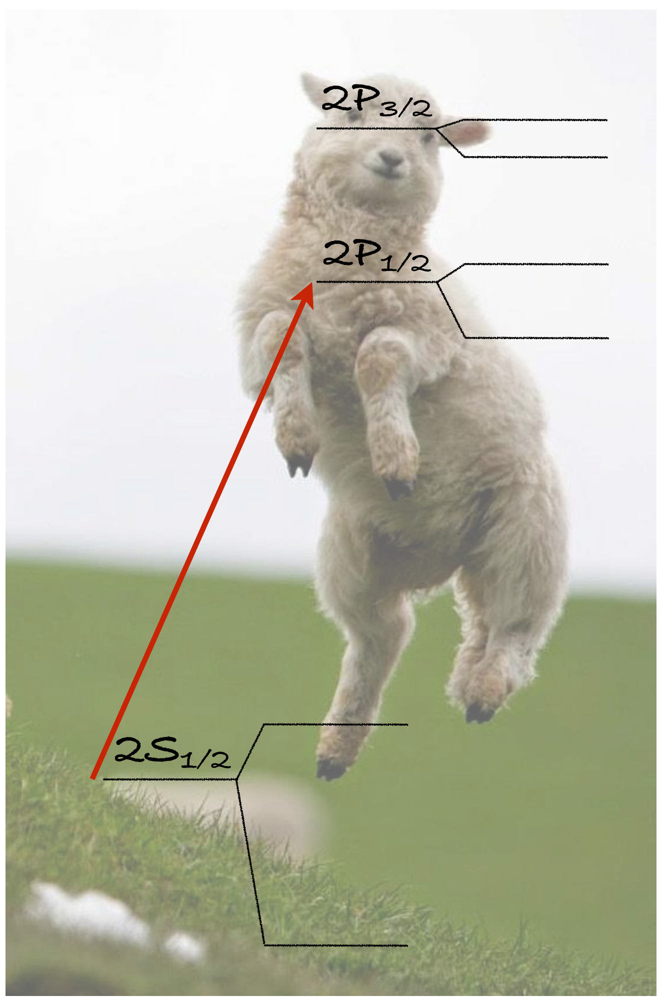

normal hydrogen:

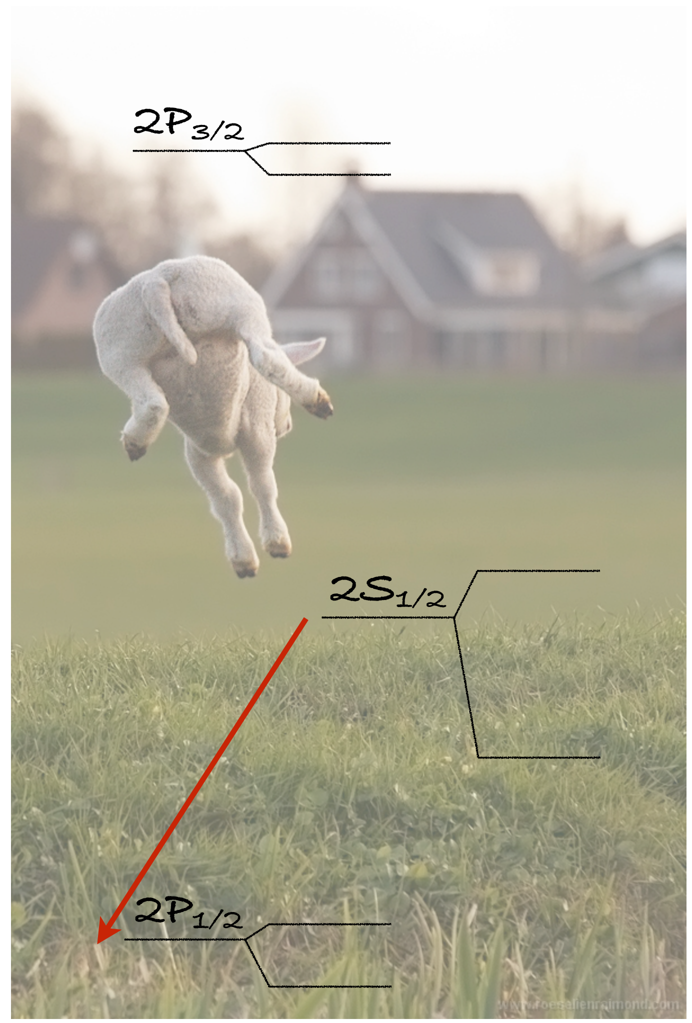

Lamb shift

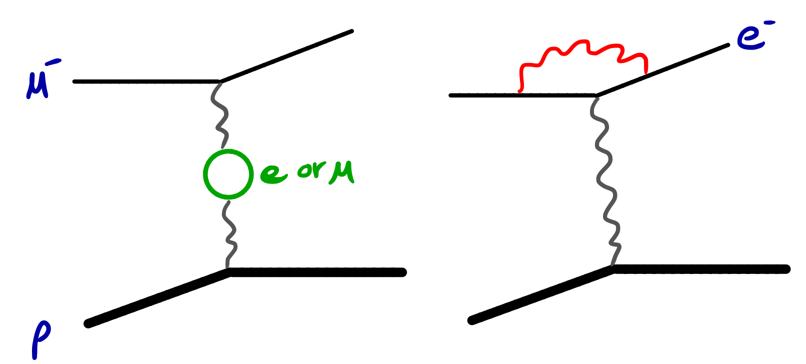

dominant QED contributions

Comprehensive theory of the Lamb shift in light muonic atoms

K. Pachucki,[1] V. Lensky,[2] F. Hagelstein,[2,3] S. S. Li Muli,[2] S. Bacca,[2,4] and R. Pohl[5]
[1] *Faculty of Physics, University of Warsaw, Pasteura 5, 02-093 Warsaw, Poland*
[2] *Institut für Kernphysik, Johannes Gutenberg-Universität Mainz, 55128 Mainz, Germany*
[3] *Paul Scherrer Institut, CH-5232 Villigen PSI, Switzerland*
[4] *Helmholtz-Institut Mainz, Johannes Gutenberg Universität Mainz, 55099 Mainz, Germany*
[5] *Institut für Physik, Johannes Gutenberg-Universität Mainz, 55099 Mainz, Germany*

(Dated: May 19, 2023) Rev. Mod. Phys. **96** (2024) 1, 015001

$E_{\rm QED}$	point nucleus	206.034 4(3)	228.774 0(3)	1644.348(8)	1668.491(7)
$\mathcal{C}\, r_C^2$	finite size	$-5.225\,9\, r_p^2$	$-6.107\,4\, r_d^2$	$-103.383\, r_h^2$	$-106.209\, r_\alpha^2$
$E_{\rm NS}$	nuclear structure	0.028 9(25)	1.750 3(200)	15.499(378)	9.276(433)
$E_L(\exp)$	experiment[a]	202.370 6(23)	202.878 5(34)	1258.598(48)	1378.521(48)
r_C	this work	0.840 60(39)	2.127 58(78)	1.970 07(94)	1.678 6(12)
r_C	previous[a]	0.840 87(39)	2.125 62(78)	1.970 07(94)	1.678 24(83)

Comprehensive theory of the Lamb shift in light muonic atoms

K. Pachucki,[1] V. Lensky,[2] F. Hagelstein,[2,3] S. S. Li Muli,[2] S. Bacca,[2,4] and R. Pohl[5]
[1] *Faculty of Physics, University of Warsaw, Pasteura 5, 02-093 Warsaw, Poland*
[2] *Institut für Kernphysik, Johannes Gutenberg-Universität Mainz, 55128 Mainz, Germany*
[3] *Paul Scherrer Institut, CH-5232 Villigen PSI, Switzerland*
[4] *Helmholtz-Institut Mainz, Johannes Gutenberg Universität Mainz, 55099 Mainz, Germany*
[5] *Institut für Physik, Johannes Gutenberg-Universität Mainz, 55099 Mainz, Germany*

(Dated: May 19, 2023) Rev. Mod. Phys. **96** (2024) 1, 015001

E_{QED}	point nucleus	206.034 4(3)	228.774 0(3)	1644.348(8)	1668.491(7)
$\mathcal{C}\, r_C^2$	finite size	$-5.225\,9\, r_p^2$	$-6.107\,4\, r_d^2$	$-103.383\, r_h^2$	$-106.209\, r_\alpha^2$
E_{NS}	nuclear structure	0.028 9(25)	1.750 3(200)	15.499(378)	9.276(433)
$E_L(\mathrm{exp})$	experiment[a]	202.370 6(23)	202.878 5(34)	1258.598(48)	1378.521(48)
r_C	this work	0.840 60(39)	2.127 58(78)	1.970 07(94)	1.678 6(12)
r_C	previous[a]	0.840 87(39)	2.125 62(78)	1.970 07(94)	1.678 24(83)

μH: present accuracy comparable with experimental precision

μD, μ^3He^+, μ^4He^+: present accuracy factor 5-10 worse than experimental precision

Comprehensive theory of the Lamb shift in light muonic atoms

K. Pachucki,[1] V. Lensky,[2] F. Hagelstein,[2,3] S. S. Li Muli,[2] S. Bacca,[2,4] and R. Pohl[5]
[1] *Faculty of Physics, University of Warsaw, Pasteura 5, 02-093 Warsaw, Poland*
[2] *Institut für Kernphysik, Johannes Gutenberg-Universität Mainz, 55128 Mainz, Germany*
[3] *Paul Scherrer Institut, CH-5232 Villigen PSI, Switzerland*
[4] *Helmholtz-Institut Mainz, Johannes Gutenberg Universität Mainz, 55099 Mainz, Germany*
[5] *Institut für Physik, Johannes Gutenberg-Universität Mainz, 55099 Mainz, Germany*

(Dated: May 19, 2023) Rev. Mod. Phys. **96** (2024) 1, 015001

$E_{\rm QED}$	point nucleus	206.034 4(3)	228.774 0(3)	1644.348(8)	1668.491(7)
$\mathcal{C}\, r_C^2$	finite size	$-5.225\,9\, r_p^2$	$-6.107\,4\, r_d^2$	$-103.383\, r_h^2$	$-106.209\, r_\alpha^2$
$E_{\rm NS}$	nuclear structure	0.028 9(25)	1.750 3(200)	15.499(378)	9.276(433)
$E_L(\exp)$	experiment[a]	202.370 6(23)	202.878 5(34)	1258.598(48)	1378.521(48)
r_C	this work	0.840 60(39)	2.127 58(78)	1.970 07(94)	1.678 6(12)
r_C	previous[a]	0.840 87(39)	2.125 62(78)	1.970 07(94)	1.678 24(83)

μH: present accuracy comparable with experimental precision

μD, μ^3He$^+$, μ^4He$^+$: present accuracy factor 5-10 worse than experimental precision

- Experiments will improve by up to a factor of 5
- Theoretical improvement needed for nuclear/nucleon 2- and 3-photon exchange

Comprehensive theory of the Lamb shift in light muonic atoms

K. Pachucki,[1] V. Lensky,[2] F. Hagelstein,[2,3] S. S. Li Muli,[2] S. Bacca,[2,4] and R. Pohl[5]
[1] *Faculty of Physics, University of Warsaw, Pasteura 5, 02-093 Warsaw, Poland*
[2] *Institut für Kernphysik, Johannes Gutenberg-Universität Mainz, 55128 Mainz, Germany*
[3] *Paul Scherrer Institut, CH-5232 Villigen PSI, Switzerland*
[4] *Helmholtz-Institut Mainz, Johannes Gutenberg Universität Mainz, 55099 Mainz, Germany*
[5] *Institut für Physik, Johannes Gutenberg-Universität Mainz, 55099 Mainz, Germany*

(Dated: May 19, 2023) Rev. Mod. Phys. **96** (2024) 1, 015001

E_{QED}	point nucleus	206.034 4(3)	228.774 0(3)	1644.348(8)	1668.491(7)
$\mathcal{C}\, r_C^2$	finite size	$-5.225\,9\, r_p^2$	$-6.107\,4\, r_d^2$	$-103.383\, r_h^2$	$-106.209\, r_\alpha^2$
E_{NS}	nuclear structure	0.028 9(25)	1.750 3(200)	15.499(378)	9.276(433)
$E_L(\mathrm{exp})$	experiment[a]	202.370 6(23)	202.878 5(34)	1258.598(48)	1378.521(48)
r_C	this work	0.840 60(39)	2.127 58(78)	1.970 07(94)	1.678 6(12)
r_C	previous[a]	0.840 87(39)	2.125 62(78)	1.970 07(94)	1.678 24(83)

$(Z\alpha)^5$	TPE	0.029 2(25)	1.979(20)	16.38(31)	9.76(40)
$\alpha^2(Z\alpha)^4$	Coulomb distortion	0.0	−0.261	−1.010	−0.536
$(Z\alpha)^6$	3PE	−0.001 3(3)	0.002 2(9)	−0.214(214)	−0.165(165)
$\alpha\,(Z\alpha)^5$	$\mathrm{eVP}^{(1)}$ with TPE	0.000 6(1)	0.027 5(4)	0.266(24)	0.158(12)
$\alpha\,(Z\alpha)^5$	$\mu\mathrm{SE}^{(1)} + \mu\mathrm{VP}^{(1)}$ with TPE	0.000 4	0.002 6(3)	0.077(8)	0.059(6)

- Theoretical improvement needed for nuclear/nucleon 2- and 3-photon exchange

STRUCTURE EFFECTS THROUGH 2γ

- Proton-structure effects at subleading orders arise through multi-photon processes

forward
two-photon exchange (2γ)

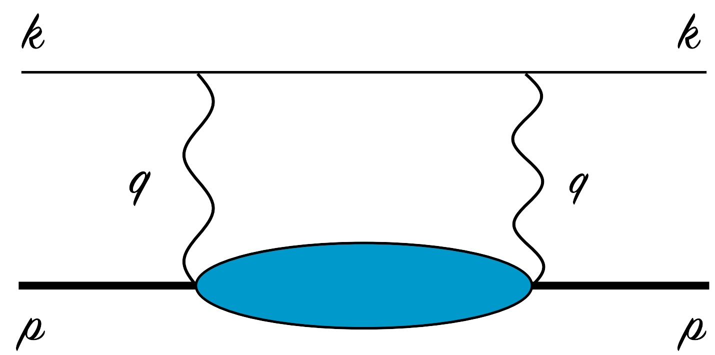

polarizability contribution
(non-Born VVCS)

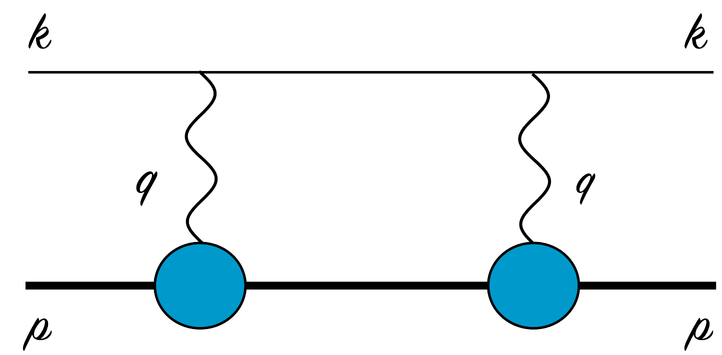

elastic contribution:
finite-size recoil,
3rd Zemach moment (Lamb shift),
Zemach radius (Hyperfine splitting)

STRUCTURE EFFECTS THROUGH 2γ

- Proton-structure effects at subleading orders arise through multi-photon processes

forward two-photon exchange (2γ)

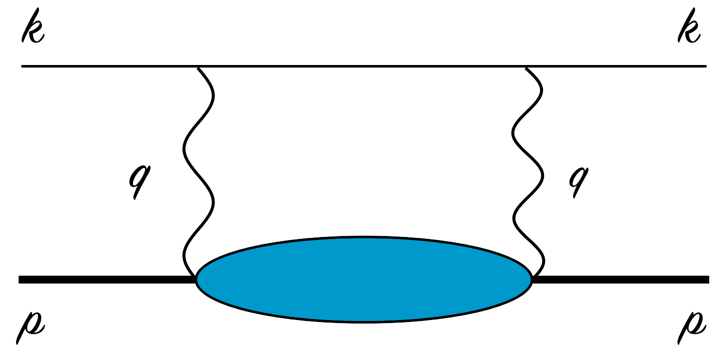

polarizability contribution
(non-Born VVCS)

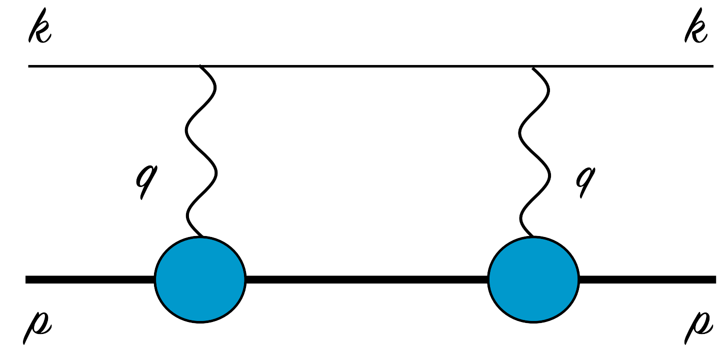

elastic contribution:
finite-size recoil,
3rd Zemach moment (Lamb shift),
Zemach radius (Hyperfine splitting)

- "Blob" corresponds to doubly-virtual Compton scattering (VVCS):

$$T^{\mu\nu}(q,p) = \left(-g^{\mu\nu} + \frac{q^\mu q^\nu}{q^2}\right) \boxed{T_1(\nu,Q^2)} + \frac{1}{M^2}\left(p^\mu - \frac{p\cdot q}{q^2}\,q^\mu\right)\left(p^\nu - \frac{p\cdot q}{q^2}\,q^\nu\right)\boxed{T_2(\nu,Q^2)}$$
$$-\frac{1}{M}\gamma^{\mu\nu\alpha}q_\alpha \boxed{S_1(\nu,Q^2)} - \frac{1}{M^2}\left(\gamma^{\mu\nu}q^2 + q^\mu\gamma^{\nu\alpha}q_\alpha - q^\nu\gamma^{\mu\alpha}q_\alpha\right)\boxed{S_2(\nu,Q^2)}$$

STRUCTURE EFFECTS THROUGH 2γ

- Proton-structure effects at subleading orders arise through multi-photon processes

forward
two-photon exchange (2γ)

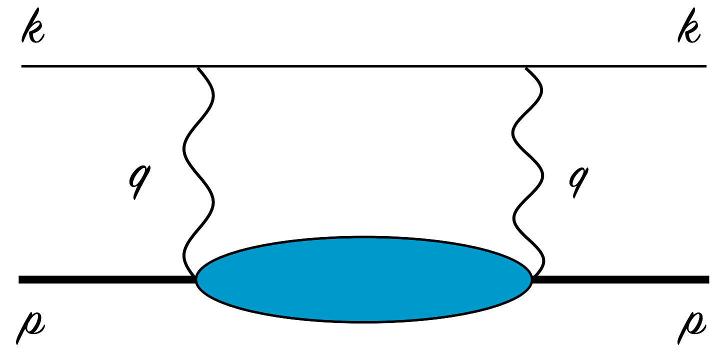

polarizability contribution
(non-Born VVCS)

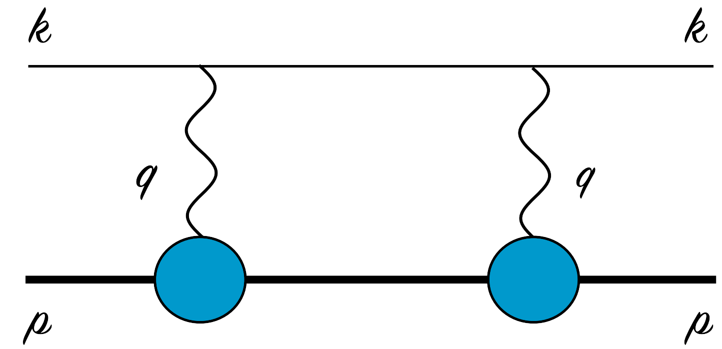

elastic contribution:
finite-size recoil,
3rd Zemach moment (Lamb shift),
Zemach radius (Hyperfine splitting)

- "Blob" corresponds to doubly-virtual Compton scattering (VVCS):

$$T^{\mu\nu}(q,p) = \left(-g^{\mu\nu} + \frac{q^\mu q^\nu}{q^2}\right) \boxed{T_1(\nu,Q^2)} + \frac{1}{M^2}\left(p^\mu - \frac{p\cdot q}{q^2}\,q^\mu\right)\left(p^\nu - \frac{p\cdot q}{q^2}\,q^\nu\right)\boxed{T_2(\nu,Q^2)}$$
$$- \frac{1}{M}\gamma^{\mu\nu\alpha} q_\alpha \boxed{S_1(\nu,Q^2)} - \frac{1}{M^2}\left(\gamma^{\mu\nu} q^2 + q^\mu \gamma^{\nu\alpha} q_\alpha - q^\nu \gamma^{\mu\alpha} q_\alpha\right)\boxed{S_2(\nu,Q^2)}$$

- Proton structure functions: $\boxed{f_1(x,Q^2),\ f_2(x,Q^2)}$, $\boxed{g_1(x,Q^2),\ g_2(x,Q^2)}$

Lamb shift — Hyperfine splitting (HFS)

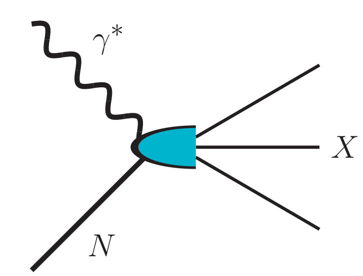

POLARIZABILITIES

Electric polarizability:

$$\vec{P} = \alpha_{E1}\,\vec{E}$$

induced electric dipole polarization (linear dielectric)

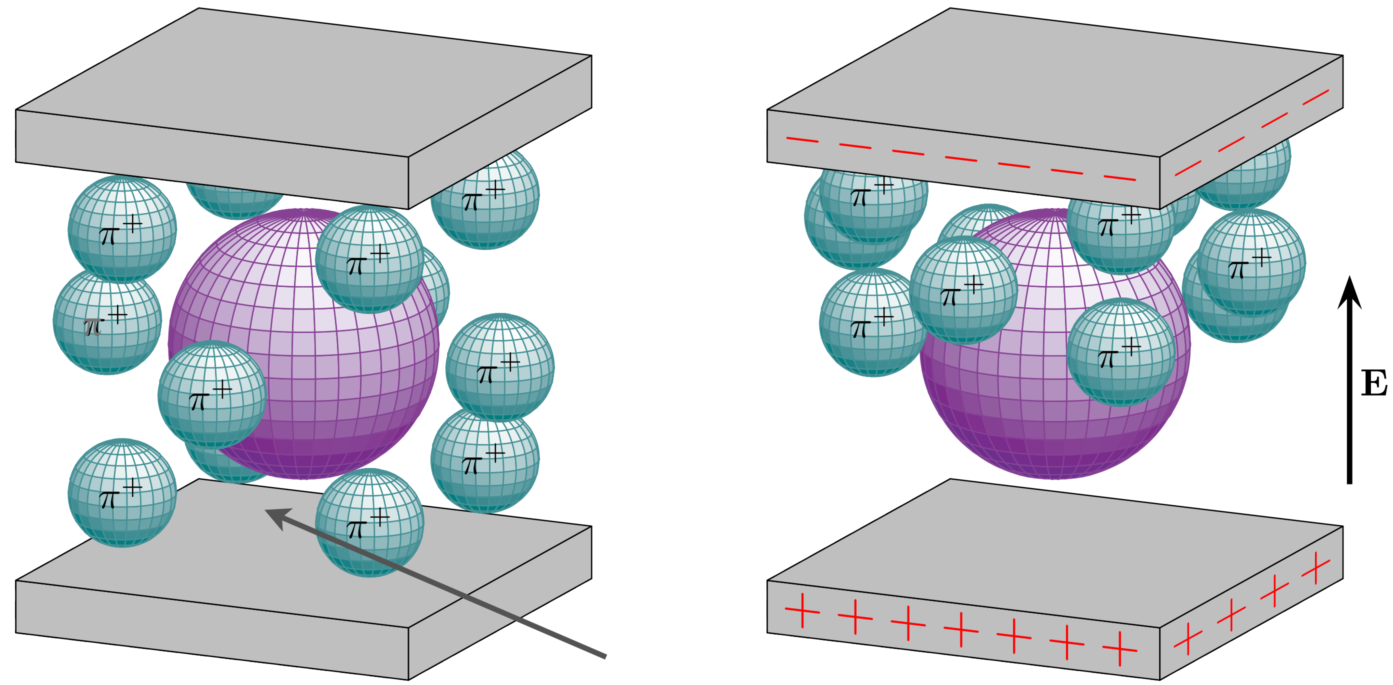

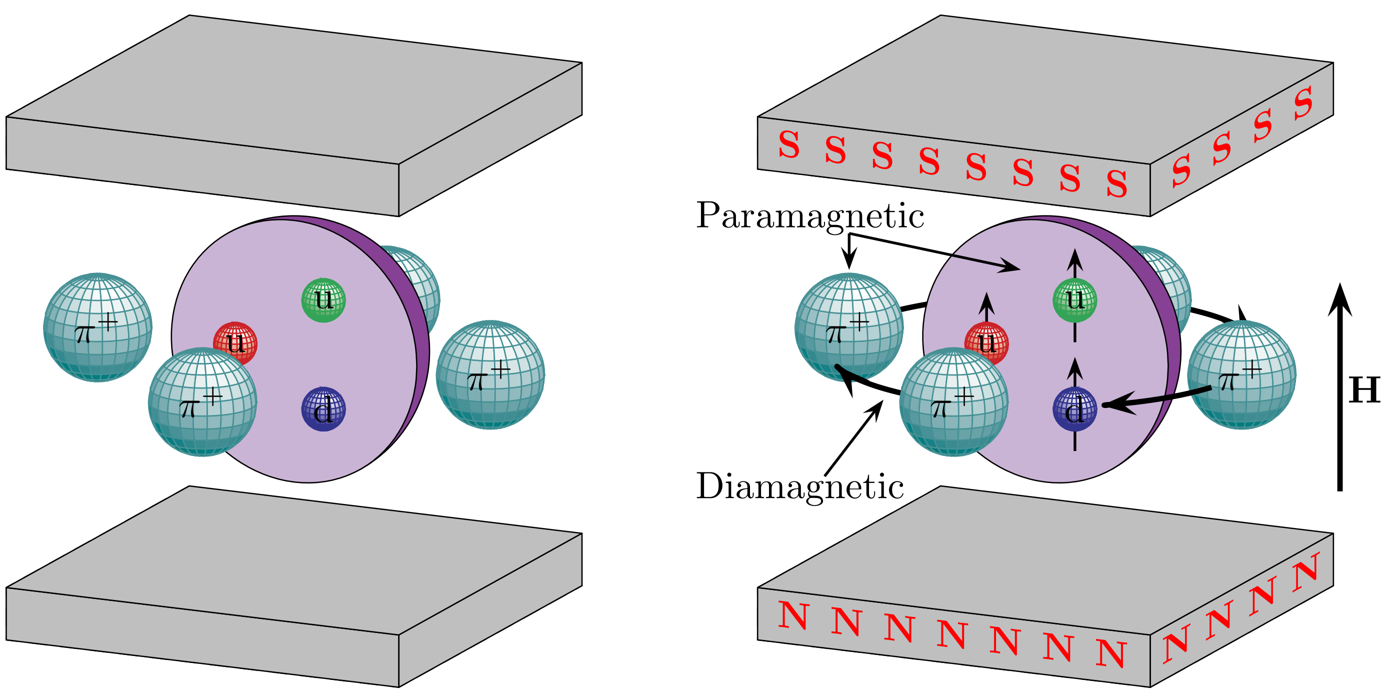

Magnetic polarizability:

$$\vec{P} = \beta_{M1}\vec{H}$$

for polarization induced by magnetic field

diamagnetic: $\beta_{M1} < 0$

paramagnetic: $\beta_{M1} > 0$

N. Sparveris, Wed.
T. Esser, Mon.

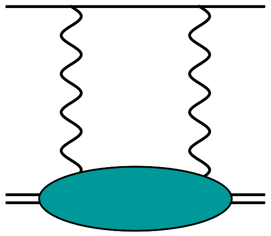

2γ EFFECT IN THE LAMB SHIFT

wave function at the origin

$$\Delta E(nS) = 8\pi\alpha m\,\phi_n^2\,\frac{1}{i}\int_{-\infty}^{\infty}\frac{\mathrm{d}\nu}{2\pi}\int\frac{\mathrm{d}\mathbf{q}}{(2\pi)^3}\,\frac{\left(Q^2-2\nu^2\right)T_1(\nu,Q^2)-(Q^2+\nu^2)\,T_2(\nu,Q^2)}{Q^4(Q^4-4m^2\nu^2)}$$

dispersion relation & optical theorem:

$$T_1(\nu,Q^2) = T_1(0,Q^2) + \frac{32\pi Z^2\alpha M\nu^2}{Q^4}\int_0^1 \mathrm{d}x\,\frac{x f_1(x,Q^2)}{1-x^2(\nu/\nu_{\mathrm{el}})^2 - i0^+}$$

$$T_2(\nu,Q^2) = \frac{16\pi Z^2\alpha M}{Q^2}\int_0^1 \mathrm{d}x\,\frac{f_2(x,Q^2)}{1-x^2(\nu/\nu_{\mathrm{el}})^2 - i0^+}$$

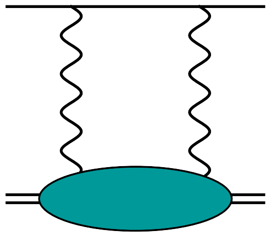

2γ EFFECT IN THE LAMB SHIFT

wave function at the origin

$$\Delta E(nS) = 8\pi\alpha m\,\phi_n^2\,\frac{1}{i}\int_{-\infty}^{\infty}\frac{\mathrm{d}\nu}{2\pi}\int\frac{\mathrm{d}\mathbf{q}}{(2\pi)^3}\frac{\left(Q^2-2\nu^2\right)T_1(\nu,Q^2)-\left(Q^2+\nu^2\right)T_2(\nu,Q^2)}{Q^4(Q^4-4m^2\nu^2)}$$

dispersion relation & optical theorem:

$$T_1(\nu,Q^2) = \boxed{T_1(0,Q^2)} + \frac{32\pi Z^2\alpha M\nu^2}{Q^4}\int_0^1 \mathrm{d}x\,\frac{x f_1(x,Q^2)}{1-x^2(\nu/\nu_{\mathrm{el}})^2-i0^+}$$

$$T_2(\nu,Q^2) = \frac{16\pi Z^2\alpha M}{Q^2}\int_0^1 \mathrm{d}x\,\frac{f_2(x,Q^2)}{1-x^2(\nu/\nu_{\mathrm{el}})^2-i0^+}$$

- Caution: in the data-driven dispersive approach the $T_1(0,Q^2)$ subtraction function is modelled!

low-energy expansion:

$$\lim_{Q^2\to 0}\overline{T}_1(0,Q^2)/Q^2 = 4\pi\beta_{M1}$$

modelled Q^2 behavior:

$$\overline{T}_1(0,Q^2) = 4\pi\beta_{M1}\,Q^2/\left(1+Q^2/\Lambda^2\right)^4$$

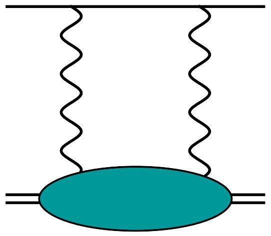

2γ EFFECT IN THE LAMB SHIFT

wave function at the origin

$$\Delta E(nS) = 8\pi\alpha m\, \phi_n^2\, \frac{1}{i}\int_{-\infty}^{\infty}\frac{d\nu}{2\pi}\int\frac{d\mathbf{q}}{(2\pi)^3}\frac{\left(Q^2-2\nu^2\right)T_1(\nu,Q^2)-\left(Q^2+\nu^2\right)T_2(\nu,Q^2)}{Q^4(Q^4-4m^2\nu^2)}$$

dispersion relation & optical theorem:

$$T_1(\nu,Q^2) = \boxed{T_1(0,Q^2)} + \frac{32\pi Z^2\alpha M\nu^2}{Q^4}\int_0^1 dx\,\frac{x f_1(x,Q^2)}{1-x^2(\nu/\nu_{el})^2-i0^+}$$

$$T_2(\nu,Q^2) = \frac{16\pi Z^2\alpha M}{Q^2}\int_0^1 dx\,\frac{f_2(x,Q^2)}{1-x^2(\nu/\nu_{el})^2-i0^+}$$

- Caution: in the data-driven dispersive approach the $T_1(0,Q^2)$ subtraction function is modelled!

low-energy expansion:

$$\lim_{Q^2\to 0}\overline{T}_1(0,Q^2)/Q^2 = 4\pi\beta_{M1}$$

modelled Q^2 behavior:

$$\overline{T}_1(0,Q^2) = 4\pi\beta_{M1}\,Q^2/\left(1+Q^2/\Lambda^2\right)^4$$

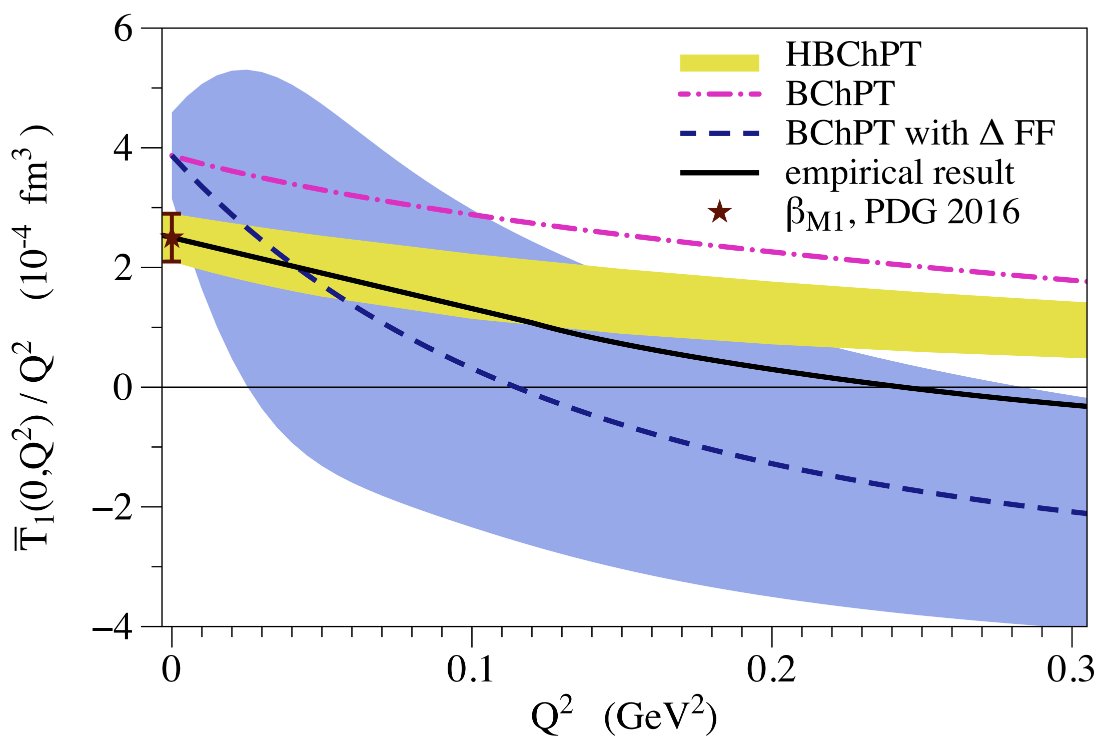

2γ POLARIZABILITY EFFECT FROM BCHPT

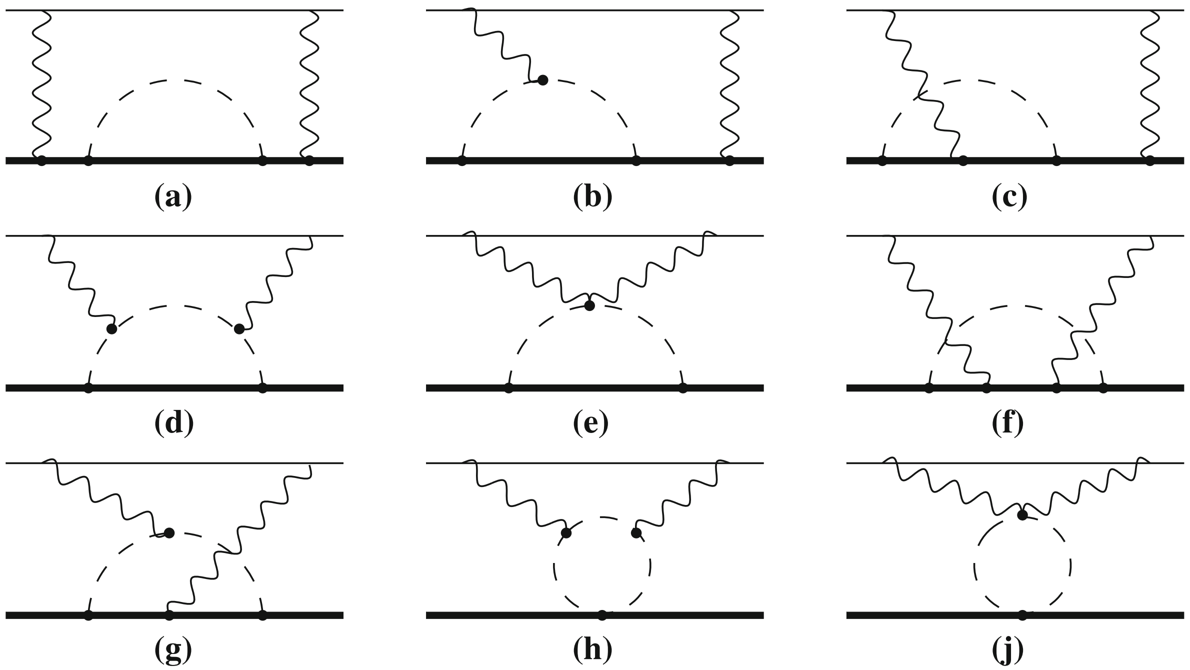

J. M. Alarcon, V. Lensky, V. Pascalutsa, Eur. Phys. J. C **74** (2014) 2852

- LO BChPT prediction with pion-nucleon loop diagrams:

$$\Delta E^{\langle \mathrm{LO} \rangle \mathrm{pol}}(2S, \mu\mathrm{H}) = -\,9.6^{+1.4}_{-2.9}\,\mu\mathrm{eV}$$

2γ POLARIZABILITY EFFECT FROM BCHPT

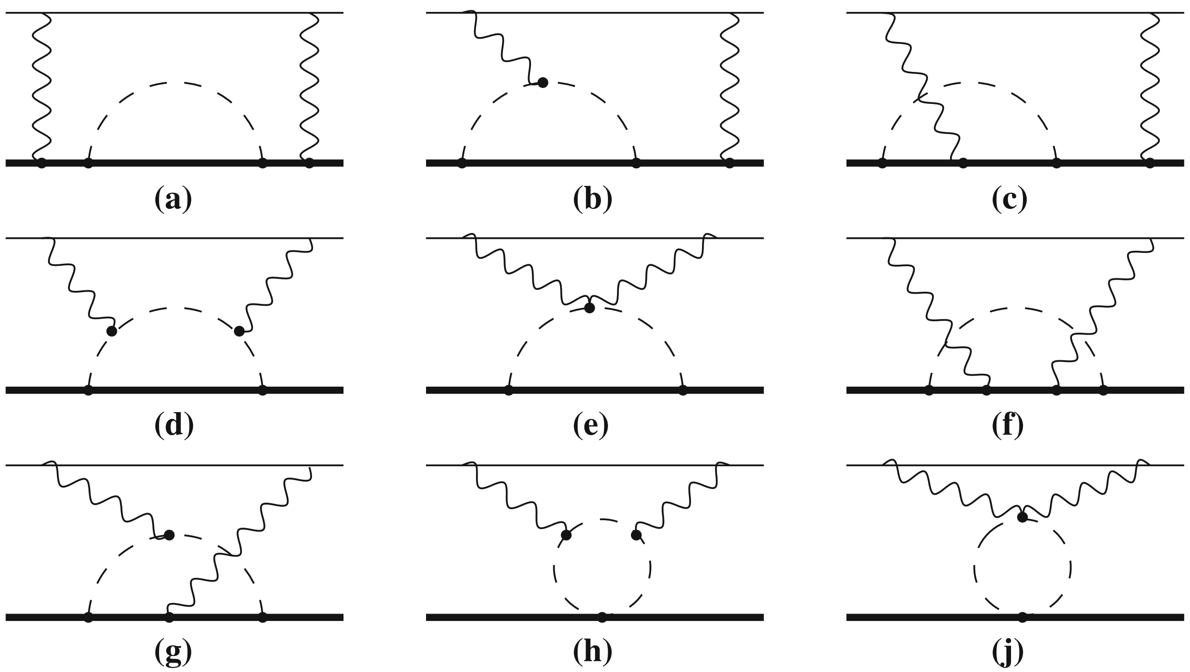

J. M. Alarcon, V. Lensky, V. Pascalutsa, Eur. Phys. J. C **74** (2014) 2852

- LO BChPT prediction with pion-nucleon loop diagrams:

$$\Delta E^{\langle \mathrm{LO}\rangle \mathrm{pol}}(2S, \mu\mathrm{H}) = -\,9.6^{+1.4}_{-2.9}\,\mu\mathrm{eV}$$

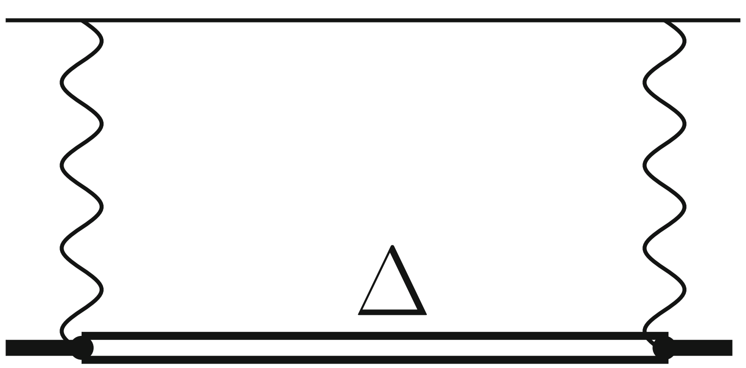

V. Lensky, FH, V. Pascalutsa, M. Vanderhaeghen, Phys. Rev. D **97** (2018) 074012

- Δ prediction from Δ(1232) exchange:
  - Uses large-N_c relations for the Jones-Scadron N-to-Δ transition form factors M. Paolone, Mon.
  - Small due to the suppression of β_{M1} in the Lamb shift but important for the T_1 subtraction function

$$\Delta E^{\langle \Delta-\mathrm{excit}\rangle \mathrm{pol}}(2S, \mu\mathrm{H}) = 0.95 \pm 0.95\,\mu\mathrm{eV}$$

POLARIZABILITY EFFECT IN μH LAMB SHIFT

Assuming ChPT is working, it should be best applicable to atomic systems, where the energies are very small !

$\propto \alpha_{E1}$

Table 1 Forward 2γ-exchange contributions to the 2S-shift in μH, in units of μeV.

Reference	$E_{2S}^{(\text{subt})}$	$E_{2S}^{(\text{inel})}$	$E_{2S}^{(\text{pol})}$	$E_{2S}^{(\text{el})}$	$E_{2S}^{\langle 2\gamma\rangle}$
DATA-DRIVEN					
(73) Pachucki '99	1.9	−13.9	−12(2)	−23.2(1.0)	−35.2(2.2)
(74) Martynenko '06	2.3	−16.1	−13.8(2.9)		
(75) Carlson *et al.* '11	5.3(1.9)	−12.7(5)	−7.4(2.0)		
(76) Birse and McGovern '12	4.2(1.0)	−12.7(5)	−8.5(1.1)	−24.7(1.6)	−33(2)
(77) Gorchtein et al.'13 [a]	−2.3(4.6)	−13.0(6)	−15.3(4.6)	−24.5(1.2)	−39.8(4.8)
(78) Hill and Paz '16					−30(13)
(79) Tomalak'18	2.3(1.3)		−10.3(1.4)	−18.6(1.6)	−29.0(2.1)
LEADING-ORDER BχPT					
(80) Alarcòn *et al.* '14			$-9.6^{+1.4}_{-2.9}$		
(81) Lensky *et al.* '17 [b]	$3.5^{+0.5}_{-1.9}$	−12.1(1.8)	$-8.6^{+1.3}_{-5.2}$		
LATTICE QCD					
(82) Fu *et al.* '22					−37.4(4.9)

[a] Adjusted values due to a different decomposition into the elastic and polarizability contributions.
[b] Partially includes the Δ(1232)-isobar contribution.

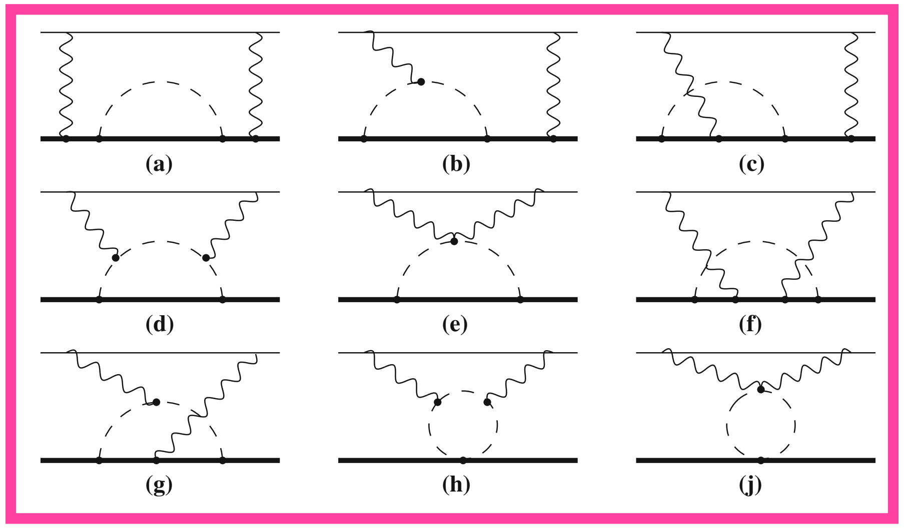

POLARIZABILITY EFFECT IN μH LAMB SHIFT

$\propto \beta_{M1}$ $\qquad$ $\propto \alpha_{E1}$

Assuming ChPT
is working, it should be best
applicable to atomic systems,
where the energies are very
small !

Table 1 Forward 2γ-exchange contributions to the $2S$-shift in μH, in units of μeV.

Reference	$E_{2S}^{(\mathrm{subt})}$	$E_{2S}^{(\mathrm{inel})}$	$E_{2S}^{(\mathrm{pol})}$	$E_{2S}^{(\mathrm{el})}$	$E_{2S}^{\langle 2\gamma\rangle}$
DATA-DRIVEN					
(73) Pachucki '99	1.9	−13.9	−12(2)	−23.2(1.0)	−35.2(2.2)
(74) Martynenko '06	2.3	−16.1	−13.8(2.9)		
(75) Carlson *et al.* '11	5.3(1.9)	−12.7(5)	−7.4(2.0)		
(76) Birse and McGovern '12	4.2(1.0)	−12.7(5)	−8.5(1.1)	−24.7(1.6)	−33(2)
(77) Gorchtein et al.'13 [a]	−2.3(4.6)	−13.0(6)	−15.3(4.6)	−24.5(1.2)	−39.8(4.8)
(78) Hill and Paz '16					−30(13)
(79) Tomalak'18	2.3(1.3)		−10.3(1.4)	−18.6(1.6)	−29.0(2.1)
LEADING-ORDER BχPT					
(80) Alarcòn *et al.* '14			$-9.6^{+1.4}_{-2.9}$		
(81) Lensky *et al.* '17 [b]	$3.5^{+0.5}_{-1.9}$	−12.1(1.8)	$-8.6^{+1.3}_{-5.2}$		
LATTICE QCD					
(82) Fu *et al.* '22					−37.4(4.9)

[a] Adjusted values due to a different decomposition into the elastic and polarizability contributions.
[b] Partially includes the $\Delta(1232)$-isobar contribution.

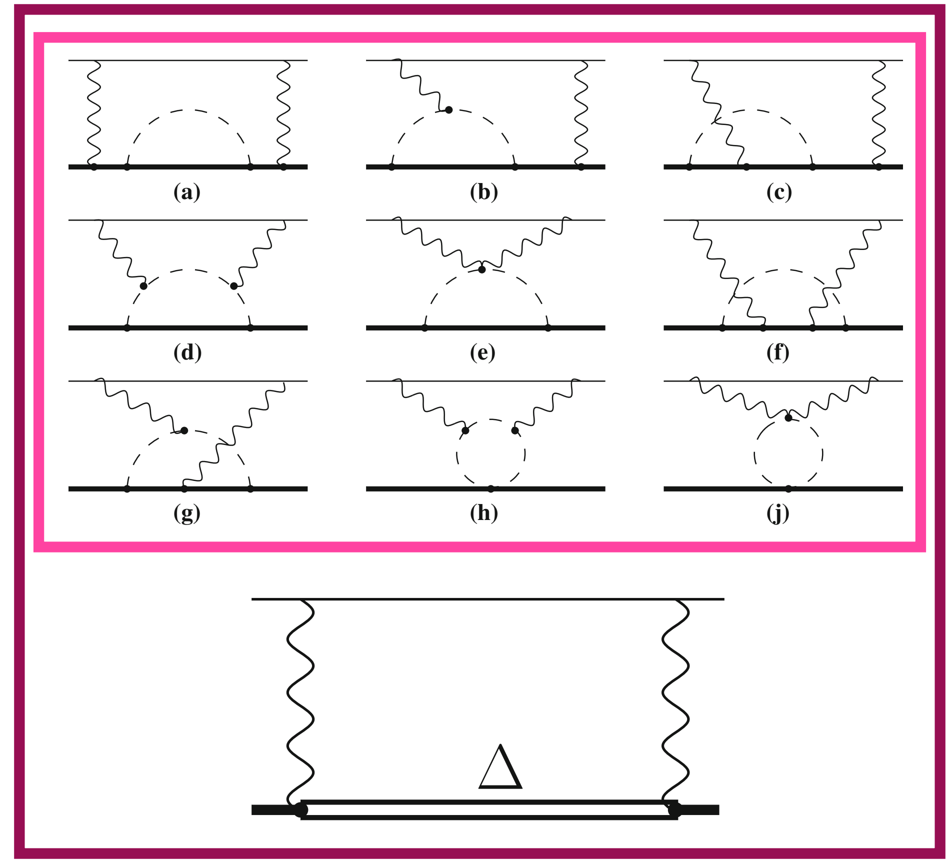

EUCLIDEAN SUBTRACTION FUNCTION

- Once-subtracted dispersion relation for $\overline{T}_1(\nu, Q^2)$ with subtraction at $\nu_s = iQ$
- Dominant part of polarizability contribution:

$$\Delta E_{nS}^{'(\text{subt})} = \frac{2\alpha m}{\pi}\phi_n^2 \int_0^\infty \frac{\text{d}Q}{Q^3}\frac{2+v_l}{(1+v_l)^2}\,\overline{T}_1(iQ,Q^2) \text{ with } v_l = \sqrt{1+4m^2/Q^2}$$

$$\overline{T}_1(iQ,Q^2) = -\overline{T}_L(iQ,Q^2) = -4\pi Q^2\alpha_{E1} + \mathcal{O}(\nu^2, Q^4)$$

- Inelastic contribution for $\nu_s = iQ$ is order of magnitude smaller than for $\nu_s = 0$
- Prospects for future lattice QCD and EFT calculations

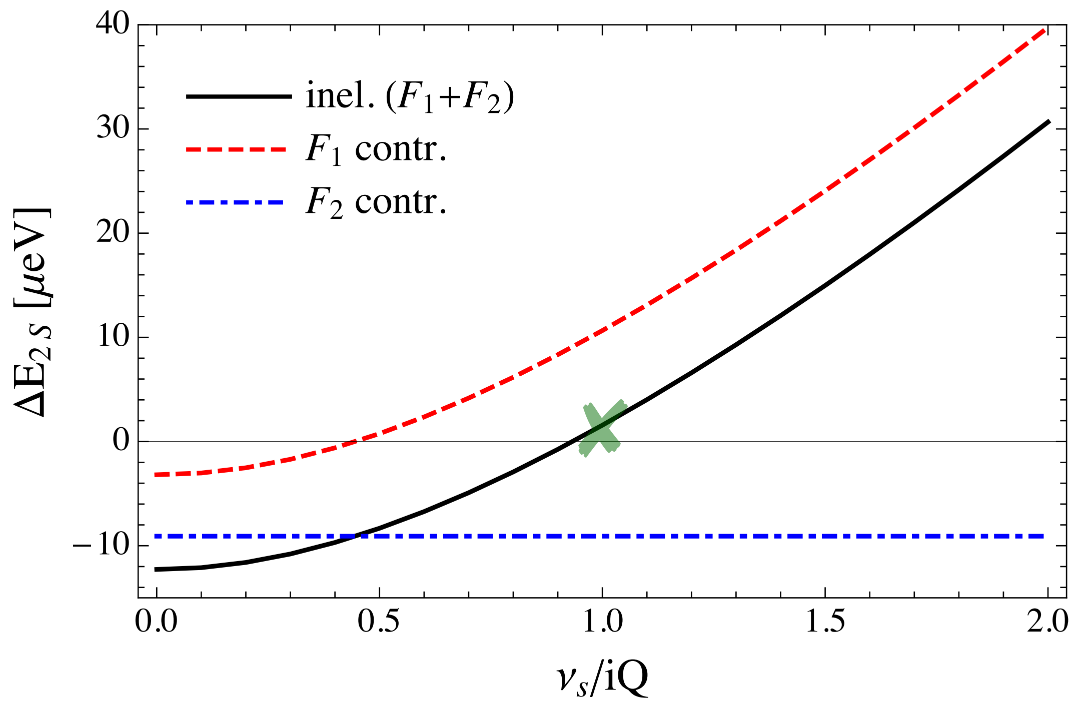

FH, V. Pascalutsa, Nucl. Phys. A **1016** (2021) 122323

based on Bosted-Christy parametrization:

$$\Delta E_{2S}^{(\text{inel})}(\nu_s = 0) \simeq -12.3\,\mu\text{eV}$$

$$\Delta E_{2S}^{'(\text{inel})}(\nu_s = iQ) \simeq 1.6\,\mu\text{eV}$$

SUBTRACTION FUNCTION

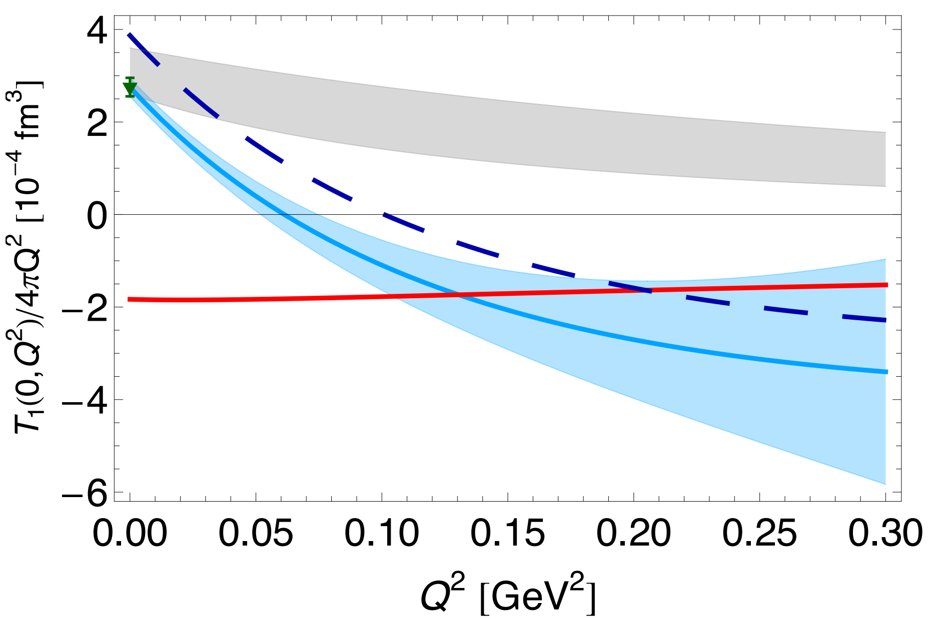

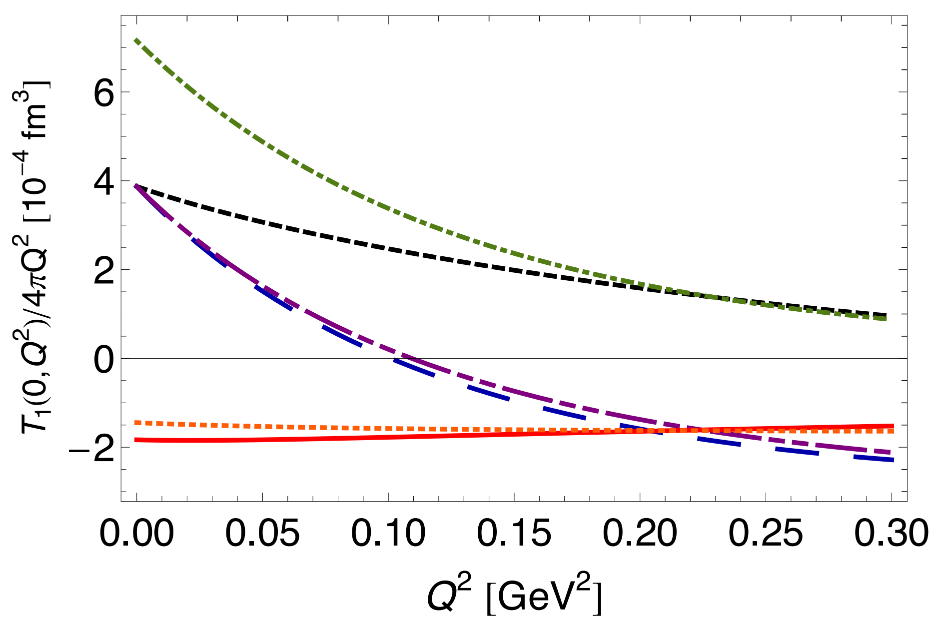

NLO BChPT δ-exp.
NLO without g_M dipole
πN loops
πΔ loops
Δ-exchange

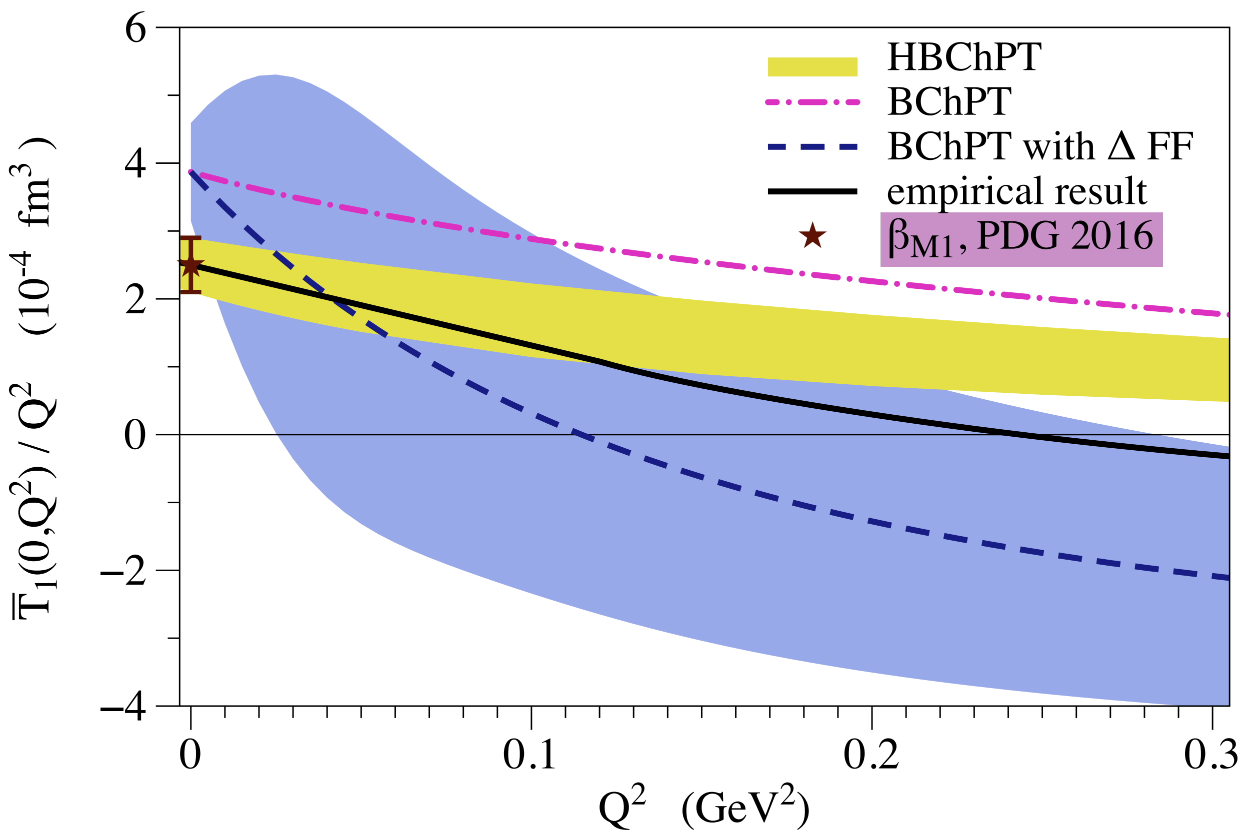

V. Lensky, FH, V. Pascalutsa and M. Vanderhaeghen
Phys. Rev. D **97** (2018) 074012

- Related to magnetic dipole polarizability:

$$\lim_{Q^2\to 0} \overline{T}_1(0,Q^2)/Q^2 = 4\pi\beta_{M1}$$

- Dominated by the Δ-exchange contribution:
  - Dipole FF on the magnetic coupling is important → zero crossing

DATA-DRIVEN EVALUATION

V. Biloshytskyi, Thu.

- New integral equations for data-driven evaluation of subtraction functions
- High-quality parametrization of σ_L at $Q \to 0$ needed

$$T_1(0,Q^2) = \frac{2Q^2}{\pi}\int_{\nu_0}^{\infty}\frac{\mathrm{d}\nu}{\nu^2+Q^2}\left[\sigma_T - \frac{\nu^2}{Q^2}\sigma_L\right](\nu,Q^2)$$

$$T_L(iQ,Q^2) = \frac{2}{\pi}\int_{\nu_0}^{\infty}\mathrm{d}\nu\,\nu^2\,\frac{\sigma_L(\nu,Q^2)}{\nu^2+Q^2}$$

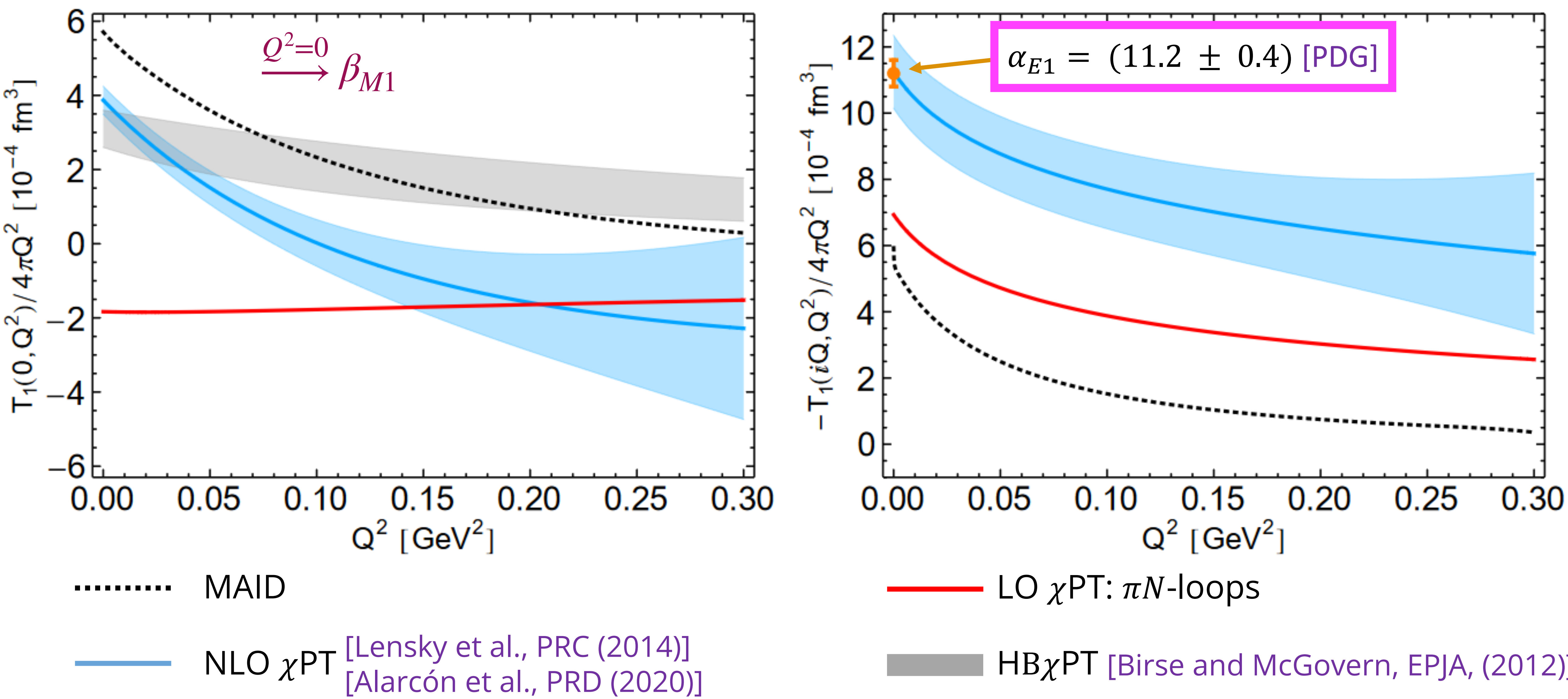

$(Z\alpha)^6 \ln(Z\alpha)$ POLARIZABILITY EFFECT

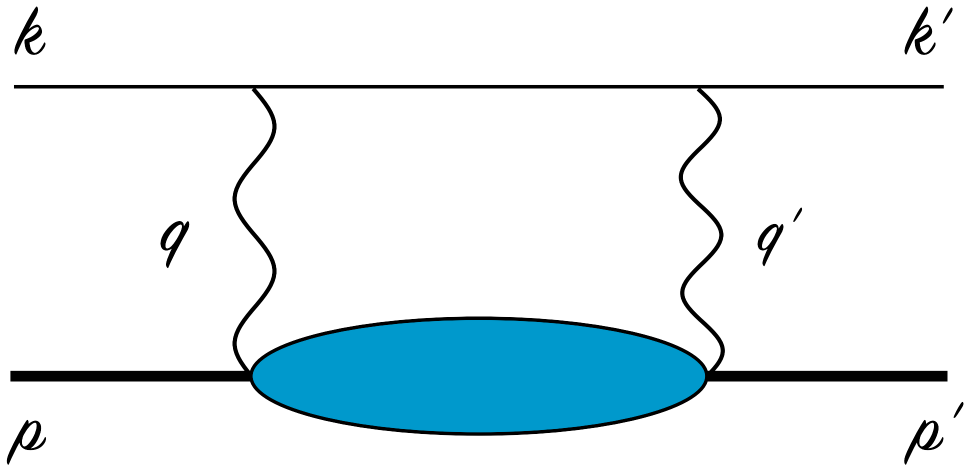

$$V(r) = \underbrace{\mathscr{M}(0)\,\delta(\boldsymbol{r})}_{\text{forward }2\gamma} - \underbrace{\frac{1}{\pi}\int_0^\infty \mathrm{d}t\ \mathrm{Im}\mathscr{M}(t)\left[\frac{\delta(\boldsymbol{r})}{t} - \frac{e^{-r\sqrt{t}}}{4\pi r}\right]}_{\text{off-forward }2\gamma}$$

forward 2γ

off-forward 2γ

$$\mathrm{Im}\,\mathscr{M}(t) \approx -\frac{\pi\alpha}{(1-t/4m^2)^{7/2}}\sqrt{t}\arccos\left[\sqrt{t}/2m\right]\alpha_{E1} + \mathcal{O}(t)$$

$$E_{nS} = -\frac{4(Z\alpha m_r)^4\alpha\,\alpha_{E1}}{n^3}\ln\frac{Z\alpha m_r}{2nm}$$

- $(Z\alpha)^6 \ln(Z\alpha)$ effect in the Lamb shift is expressed entirely in terms of the static electric dipole polarizability
- No contribution from the magnetic dipole polarizability
- Can be identified with the known Coulomb distortion effect

HYPERFINE SPLITTING IN μH

$$\Delta E_{\mathrm{HFS}}(nS) = [1 + \Delta_{\mathrm{QED}} + \Delta_{\mathrm{weak}} + \Delta_{\mathrm{structure}}]\, E_F(nS)$$

Fermi energy:

$$E_F(nS) = \frac{8}{3}\frac{Z\alpha}{a^3}\frac{1+\kappa}{mM}\frac{1}{n^3}$$

with Bohr radius $a = 1/(Z\alpha m_r)$

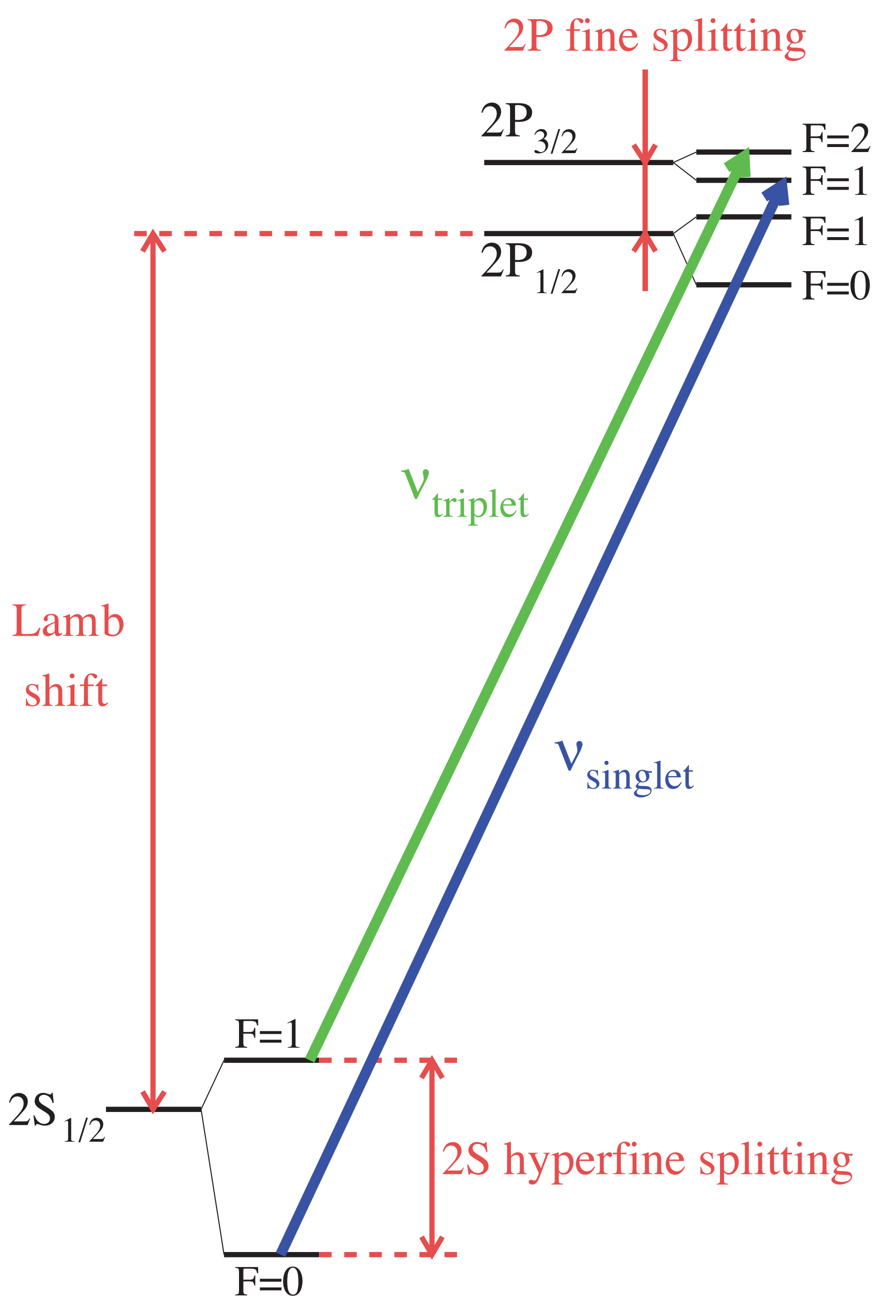

⏰ Measurements of the μH ground-state HFS planned by the CREMA and FAMU collaborations

- Very precise input for the 2γ effect needed to narrow down frequency search range for experiment
- Zemach radius can help to pin down the magnetic properties of the proton

HYPERFINE SPLITTING IN μH

$$\Delta E_{\mathrm{HFS}}(nS) = [1 + \Delta_{\mathrm{QED}} + \Delta_{\mathrm{weak}} + \Delta_{\mathrm{structure}}]\, E_F(nS)$$

with $\Delta_{\mathrm{structure}} = \Delta_Z + \Delta_{\mathrm{recoil}} + \Delta_{\mathrm{pol}}$

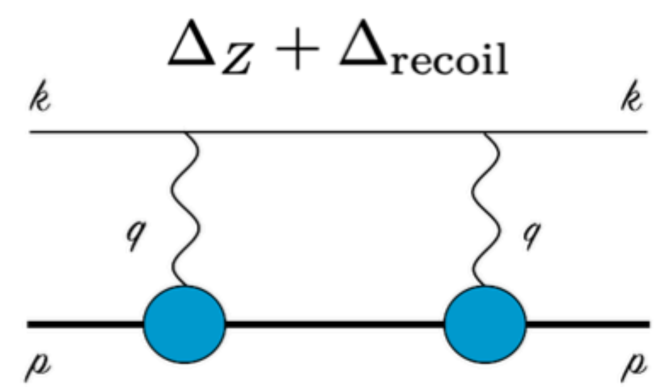

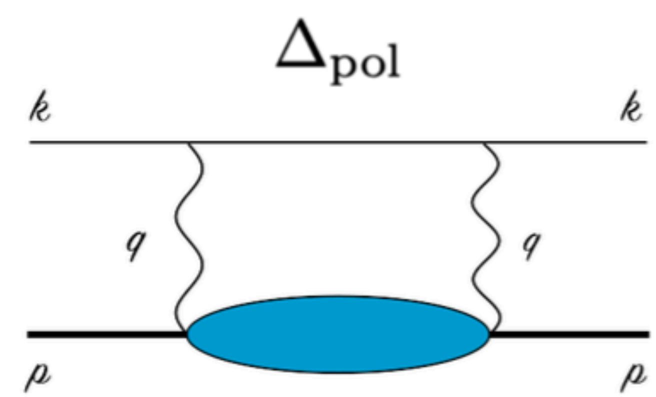

HYPERFINE SPLITTING IN μH

$$\Delta E_{\mathrm{HFS}}(nS) = \left[1 + \Delta_{\mathrm{QED}} + \Delta_{\mathrm{weak}} + \Delta_{\mathrm{structure}}\right] E_F(nS)$$

with $\Delta_{\mathrm{structure}} = \Delta_Z + \Delta_{\mathrm{recoil}} + \Delta_{\mathrm{pol}}$

Zemach radius:

$$\Delta_Z = \frac{8Z\alpha m_r}{\pi} \int_0^\infty \frac{\mathrm{d}Q}{Q^2} \left[\frac{G_E(Q^2) G_M(Q^2)}{1+\kappa} - 1\right] \equiv -2Z\alpha m_r R_Z$$

A. Antognini, et al., Science **339** (2013) 417–420

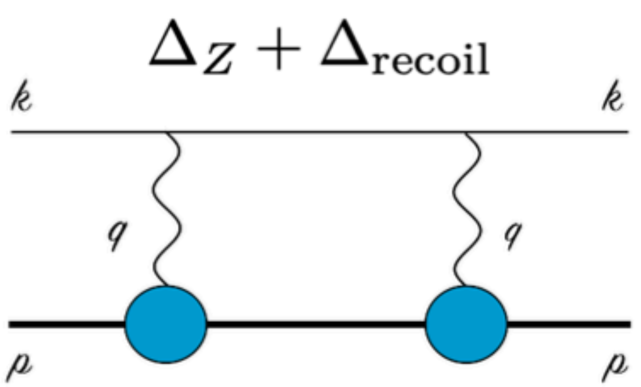

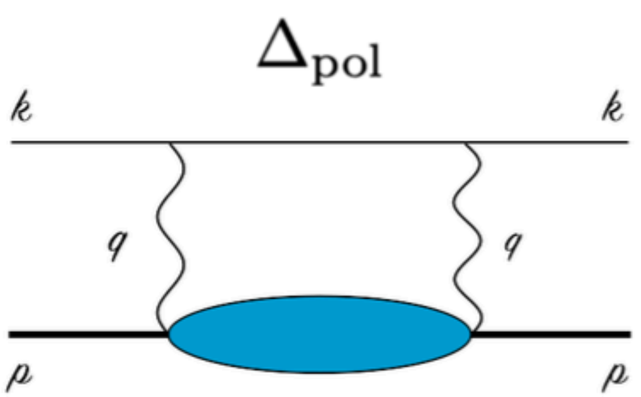

HYPERFINE SPLITTING IN μH

$$\Delta E_{\mathrm{HFS}}(nS) = [1 + \Delta_{\mathrm{QED}} + \Delta_{\mathrm{weak}} + \Delta_{\mathrm{structure}}]\, E_F(nS)$$

with $\Delta_{\mathrm{structure}} = \Delta_Z + \Delta_{\mathrm{recoil}} + \Delta_{\mathrm{pol}}$

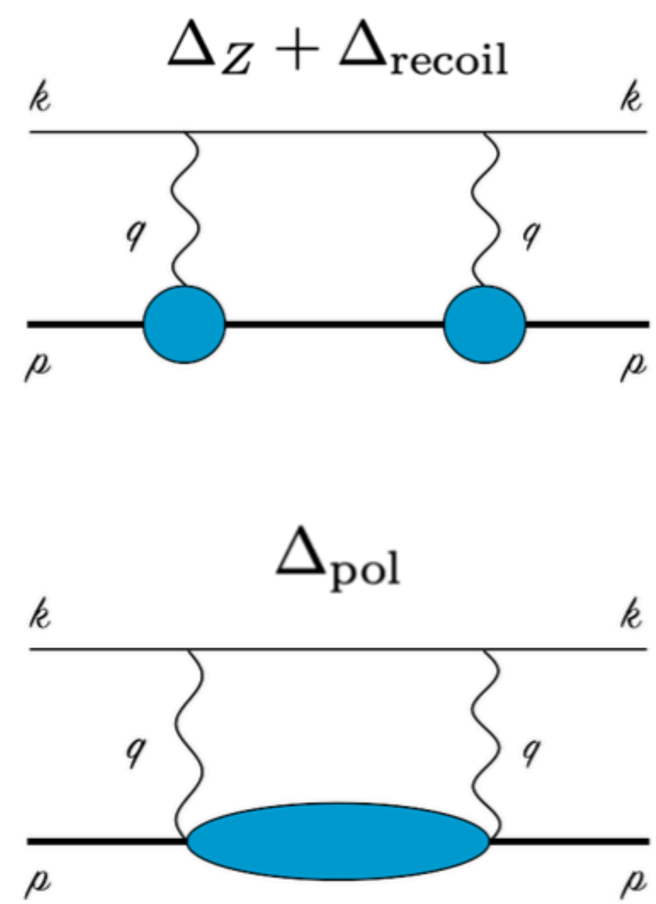

Zemach radius:

$$\Delta_Z = \frac{8Z\alpha m_r}{\pi} \int_0^\infty \frac{\mathrm{d}Q}{Q^2} \left[\frac{G_E(Q^2) G_M(Q^2)}{1+\kappa} - 1 \right] \equiv -2Z\alpha m_r R_Z$$

A. Antognini, et al., Science **339** (2013) 417–420

R_Z	Δ_Z	Δ_{recoil}	Δ_{pol}
$1.054^{+0.003}_{-0.002}$ fm	-7403^{+21}_{-16} ppm	850 ppm	37(95) ppm (LO BChPT)
[Lin, et al. '22]	[Antognini, et al. '22, annual reviews]	[Antognini, et al. '22]	[Hagelstein, et al. '23]

HYPERFINE SPLITTING IN μH

Theory: QED, ChPT, data-driven dispersion relations, ab-initio few-nucleon theories

Experiment: HFS in μH, μHe$^+$, …

Guiding the exp.

find narrow 1S HFS transitions with the help of full theory predictions: QED, weak, finite size, polarizability

Interpreting the exp.

extract E^{TPE}, $E^{\text{pol.}}$ or R_Z

Input for data-driven evaluations

form factors, structure functions, polarizabilities

Testing the theory

- discriminate between theory predictions for polarizability effect
    - disentangle R_Z & polarizability effect by combining HFS in H & μH
- test HFS theory
    - combining HFS in H & μH with theory prediction for polarizability effect
- test nuclear theories

Determine fundamental constants

Zemach radius R_Z

Spectroscopy of ordinary atoms (H, He$^+$)

Electron and Compton Scattering

TING IN μH

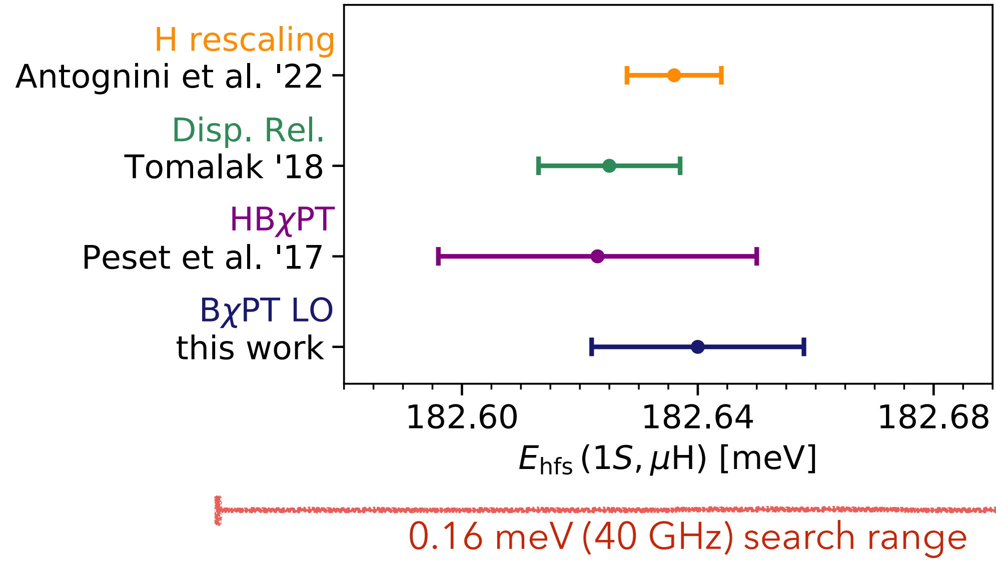

Predictions for the 1S HFS in μH are driven by the 1S HFS in H

A. Antognini, FH, V. Pascalutsa, Ann. Rev. Nucl. Part. **72** (2022)

Experiment: HFS in μH, μHe$^+$, …

Guiding the exp.

find narrow 1S HFS transitions with the help of full theory predictions: QED, weak, finite size, polarizability

Interpreting the exp.

extract $E^{\rm TPE}$, $E^{\rm pol.}$ or R_Z

Input for data-driven evaluations

form factors, structure functions, polarizabilities

esting the theory

inate between theory predictions for polarizability effect

- disentangle R_Z & polarizability effect by combining HFS in H & μH

- test HFS theory
  - combining HFS in H & μH with theory prediction for polarizability effect
- test nuclear theories

Determine fundamental constants

Zemach radius R_Z

Spectroscopy of ordinary atoms (H, He$^+$)

Electron and Compton Scattering

HYPERFINE SPLITTING IN μH

The hyperfine splitting of μH (theory update):

A. Antognini, FH, V. Pascalutsa, Ann. Rev. Nucl. Part. **72** (2022)

$$E_{1S\text{-hfs}} = \Big[\underbrace{182.443}_{E_\mathrm{F}} \underbrace{+1.350(7)}_{\text{QED+weak}} \underbrace{+0.004}_{\text{hVP}} \underbrace{-1.30653(17)\left(\frac{r_{Zp}}{\text{fm}}\right) + E_\mathrm{F}\left(1.01656(4)\,\Delta_\text{recoil} + 1.00402\,\Delta_\text{pol}\right)}_{2\gamma\text{ incl. radiative corr.}}\Big]\,\text{meV}$$

Guiding the exp.

find narrow 1S HFS transitions with the help of full theory predictions: QED, weak, finite size, polarizability

Interpreting the exp.

extract E^TPE, $E^\text{pol.}$ or R_Z

Input for data-driven evaluations

form factors, structure functions, polarizabilities

- discriminate between theory predictions for polarizability effect
  - disentangle R_Z & polarizability effect by combining HFS in H & μH
- test HFS theory
  - combining HFS in H & μH with theory prediction for polarizability effect
- test nuclear theories

Determine fundamental constants

Zemach radius R_Z

Spectroscopy of ordinary atoms (H, He$^+$)

Electron and Compton Scattering

POLARIZABILITY EFFECT IN HFS

- Polarizability effect on the HFS is completely constrained by empirical information

$$\Delta_{\text{pol.}} = \Delta_1 + \Delta_2 = \frac{\alpha m}{2\pi(1+\kappa)M}\left(\delta_1 + \delta_2\right)$$

$$\delta_1 = 2\int_0^\infty \frac{\mathrm{d}Q}{Q}\left\{\frac{5+4v_l}{(v_l+1)^2}\left[4I_1(Q^2)+F_2^2(Q^2)\right] - \frac{32M^4}{Q^4}\int_0^{x_0}\mathrm{d}x\, x^2 g_1(x,Q^2)\frac{1}{(v_l+v_x)(1+v_x)(1+v_l)}\left(4+\frac{1}{1+v_x}+\frac{1}{v_l+1}\right)\right\}$$

$$\delta_2 = 96M^2\int_0^\infty \frac{\mathrm{d}Q}{Q^3}\int_0^{x_0}\mathrm{d}x\, g_2(x,Q^2)\left(\frac{1}{v_l+v_x} - \frac{1}{v_l+1}\right)$$

with $v_l = \sqrt{1+\frac{1}{\tau_l}}$, $v_x = \sqrt{1+x^2\tau^{-1}}$, $\tau_l = \frac{Q^2}{4m^2}$ and $\tau = \frac{Q^2}{4M^2}$

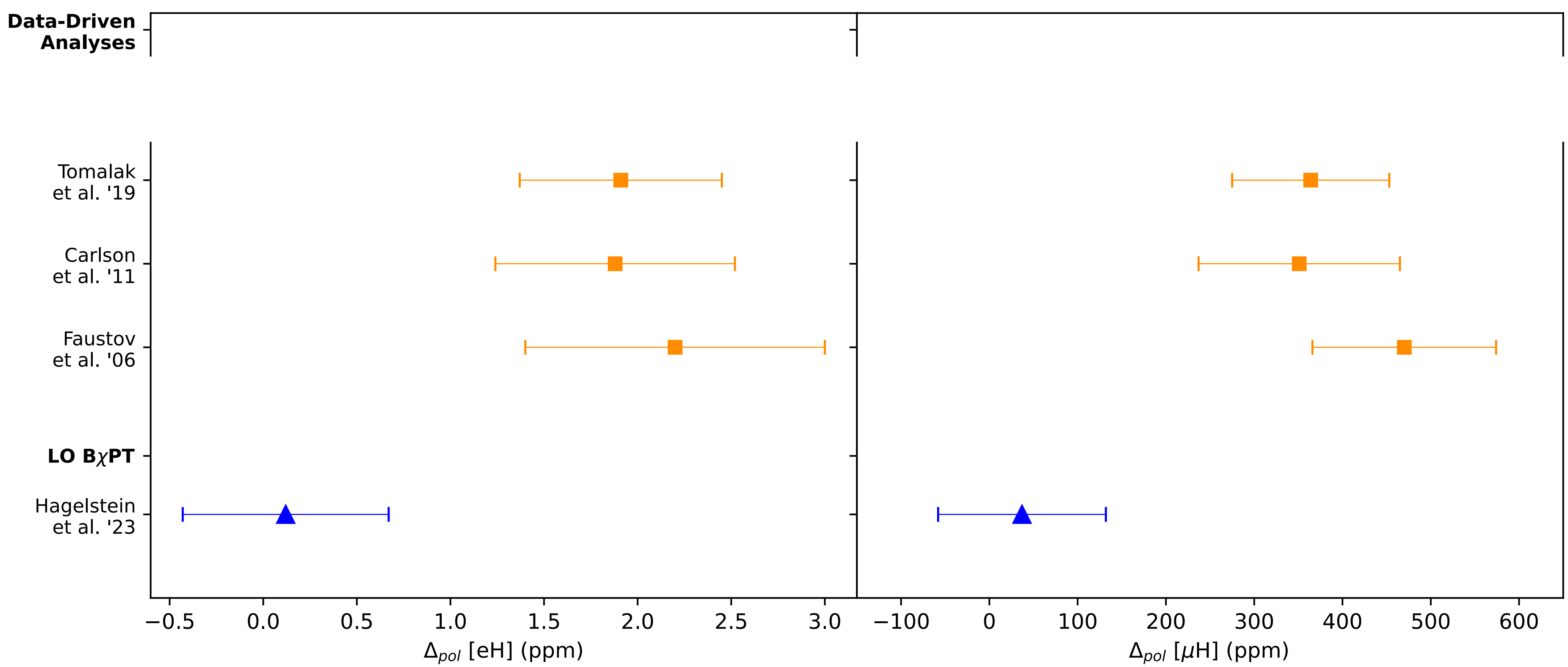

POLARIZABILITY EFFECT IN HFS

- Polarizability effect on the HFS is completely constrained by empirical information

$$\Delta_{\text{pol.}} = \Delta_1 + \Delta_2 = \frac{\alpha m}{2\pi(1+\kappa)M}\left(\delta_1+\delta_2\right)$$

$$\delta_1 = 2\int_0^\infty \frac{\mathrm{d}Q}{Q}\left\{\frac{5+4v_l}{(v_l+1)^2}\left[4I_1(Q^2)+F_2^2(Q^2)\right] - \frac{32M^4}{Q^4}\int_0^{x_0}\mathrm{d}x\, x^2 g_1(x,Q^2)\frac{1}{(v_l+v_x)(1+v_x)(1+v_l)}\left(4+\frac{1}{1+v_x}+\frac{1}{v_l+1}\right)\right\}$$

$$\delta_2 = 96M^2\int_0^\infty \frac{\mathrm{d}Q}{Q^3}\int_0^{x_0}\mathrm{d}x\, g_2(x,Q^2)\left(\frac{1}{v_l+v_x}-\frac{1}{v_l+1}\right)$$

with $v_l = \sqrt{1+\frac{1}{\tau_l}}$, $v_x = \sqrt{1+x^2\tau^{-1}}$, $\tau_l = \frac{Q^2}{4m^2}$ and $\tau = \frac{Q^2}{4M^2}$

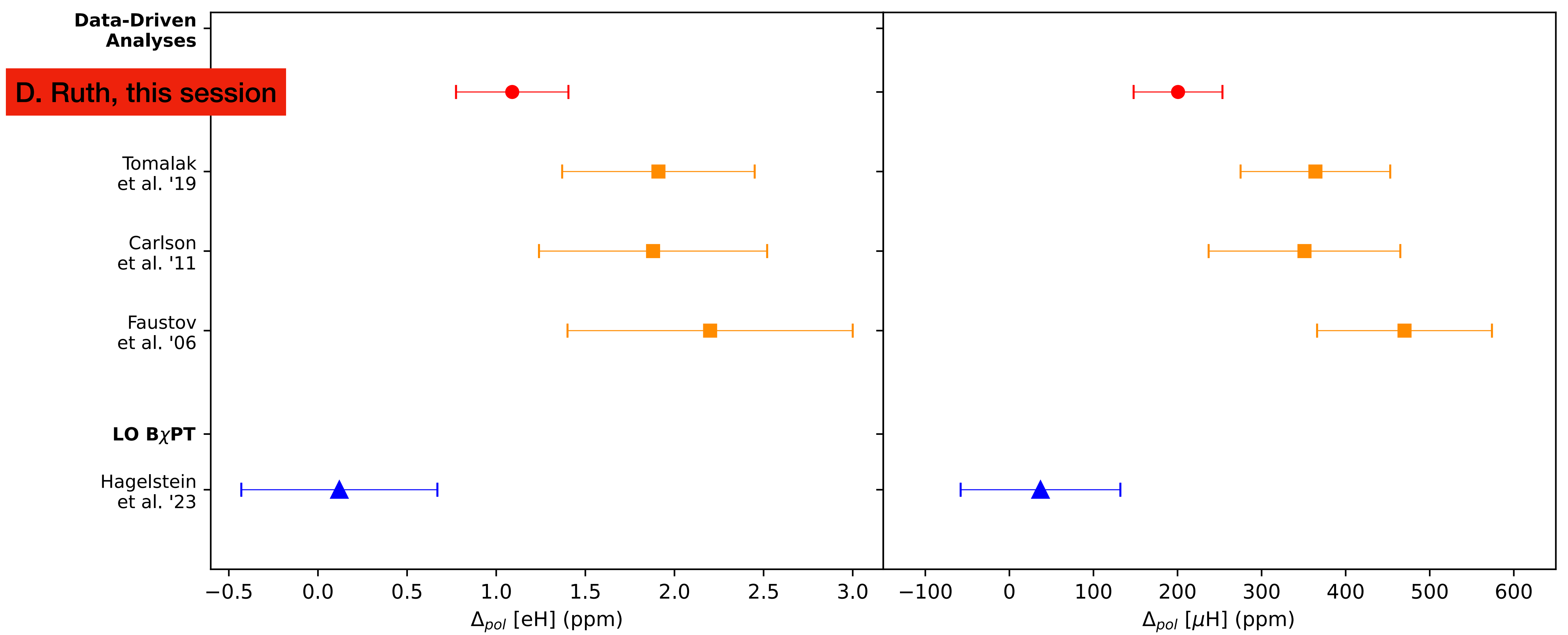

2γ EFFECT IN THE μH HFS

Table 1 Forward 2γ-exchange contribution to the HFS in μH.

Reference	Δ_Z [ppm]	Δ_{recoil} [ppm]	Δ_{pol} [ppm]	Δ_1 [ppm]	Δ_2 [ppm]	$E_{1S\text{-hfs}}^{\langle 2\gamma\rangle}$ [meV]
DATA-DRIVEN						
Pachucki '96 (1)	−8025	1666	0(658)			−1.160
Faustov et al. '01 (9)[a]	−7180		410(80)	468	−58	
Faustov et al. '06 (10)[b]			470(104)	518	−48	
Carlson et al. '11 (11)[c]	−7703	931	351(114)	370(112)	−19(19)	−1.171(39)
Tomalak '18 (12)[d]	−7333(48)	846(6)	364(89)	429(84)	−65(20)	−1.117(19)
HEAVY-BARYON χPT						
Peset et al. '17 (13)						−1.161(20)
LEADING-ORDER χPT						
Hagelstein et al. '16 (14)			37(95)	29(90)	9(29)	
+ $\Delta(1232)$ EXCIT.						
Hagelstein et al. '18 (15)			−13	84	−97	

[a] Adjusted values: Δ_{pol} and Δ_1 corrected by −46 ppm as described in Ref. 16.
[b] Different convention was used to calculate the Pauli form factor contribution to Δ_1, which is equivalent to the approximate formula in the limit of $m = 0$ used for H in Ref. 11.
[c] Elastic form factors from Ref. 17 and updated error analysis from Ref. 16. Note that this result already includes radiative corrections for the Zemach-radius contribution, $(1+\delta_Z^{rad})\Delta_Z$ with $\delta_Z^{rad} \sim 0.0153$ (18, 19), as well as higher-order recoil corrections with the proton anomalous magnetic moment, cf. (11, Eq. 22) and (18).
[d] Uses r_p from μH (20) as input.

2γ EFFECT IN THE μH HFS

Table 1 Forward 2γ-exchange contribution to the HFS in μH.

Reference	Δ_Z [ppm]	Δ_{recoil} [ppm]	Δ_{pol} [ppm]	Δ_1 [ppm]	Δ_2 [ppm]	$E^{\langle 2\gamma \rangle}_{1S\text{-hfs}}$ [meV]
DATA-DRIVEN						
Pachucki '96 (1)	−8025	1666	0(658)			−1.160
Faustov et al. '01 (9)[a]	−7180		410(80)	468	−58	
Faustov et al. '06 (10)[b]			470(104)	518	−48	
Carlson et al. '11 (11)[c]	−7703	931	351(114)	370(112)	−19(19)	−1.171(39)
Tomalak '18 (12)[d]	−7333(48)	846(6)	364(89)	429(84)	−65(20)	−1.117(19)
HEAVY-BARYON χPT						
Peset et al. '17 (13)						−1.161(20)
LEADING-ORDER χPT						
Hagelstein et al. '16 (14)			37(95)	29(90)	9(29)	
+ $\Delta(1232)$ EXCIT.						
Hagelstein et al. '18 (15)			−13	84	−97	

[a] Adjusted values: Δ_{pol} and Δ_1 corrected by −46 ppm as described in Ref. 16.
[b] Different convention was used to calculate the Pauli form factor contribution to Δ_1, which is equivalent to the approximate formula in the limit of $m = 0$ used for H in Ref. 11.
[c] Elastic form factors from Ref. 17 and updated error analysis from Ref. 16. Note that this result already includes radiative corrections for the Zemach-radius contribution, $(1+\delta_Z^{rad})\Delta_Z$ with $\delta_Z^{rad} \sim 0.0153$ (18, 19), as well as higher-order recoil corrections with the proton anomalous magnetic moment, cf. (11, Eq. 22) and (18).
[d] Uses r_p from μH (20) as input.

Assuming ChPT is working, it should be best applicable to atomic systems, where the energies are very small !

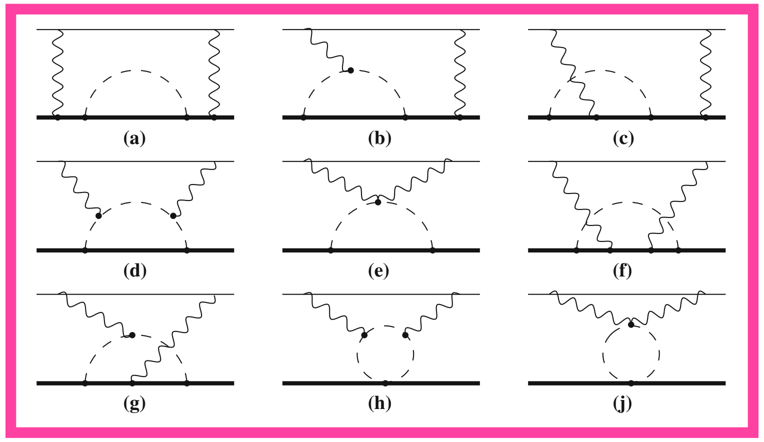

2γ EFFECT IN THE μH HFS

Table 1 Forward 2γ-exchange contribution to the HFS in μH.

Reference	Δ_Z [ppm]	Δ_{recoil} [ppm]	Δ_{pol} [ppm]	Δ_1 [ppm]	Δ_2 [ppm]	$E^{\langle 2\gamma\rangle}_{1S\text{-hfs}}$ [meV]
DATA-DRIVEN						
Pachucki '96 (1)	−8025	1666	0(658)			−1.160
Faustov et al. '01 (9)[a]	−7180		410(80)	468	−58	
Faustov et al. '06 (10)[b]			470(104)	518	−48	
Carlson et al. '11 (11)[c]	−7703	931	351(114)	370(112)	−19(19)	−1.171(39)
Tomalak '18 (12)[d]	−7333(48)	846(6)	364(89)	429(84)	−65(20)	−1.117(19)
HEAVY-BARYON χPT						
Peset et al. '17 (13)						−1.161(20)
LEADING-ORDER χPT						
Hagelstein et al. '16 (14)			37(95)	29(90)	9(29)	
+ $\Delta(1232)$ EXCIT.						
Hagelstein et al. '18 (15)			−13	84	−97	

[a] Adjusted values: Δ_{pol} and Δ_1 corrected by −46 ppm as described in Ref. 16.
[b] Different convention was used to calculate the Pauli form factor contribution to Δ_1, which is equivalent to the approximate formula in the limit of $m = 0$ used for H in Ref. 11.
[c] Elastic form factors from Ref. 17 and updated error analysis from Ref. 16. Note that this result already includes radiative corrections for the Zemach-radius contribution, $(1+\delta_Z^{\text{rad}})\Delta_Z$ with $\delta_Z^{\text{rad}} \sim 0.0153$ (18, 19), as well as higher-order recoil corrections with the proton anomalous magnetic moment, cf. (11, Eq. 22) and (18).
[d] Uses r_p from μH (20) as input.

Assuming ChPT is working, it should be best applicable to atomic systems, where the energies are very small !

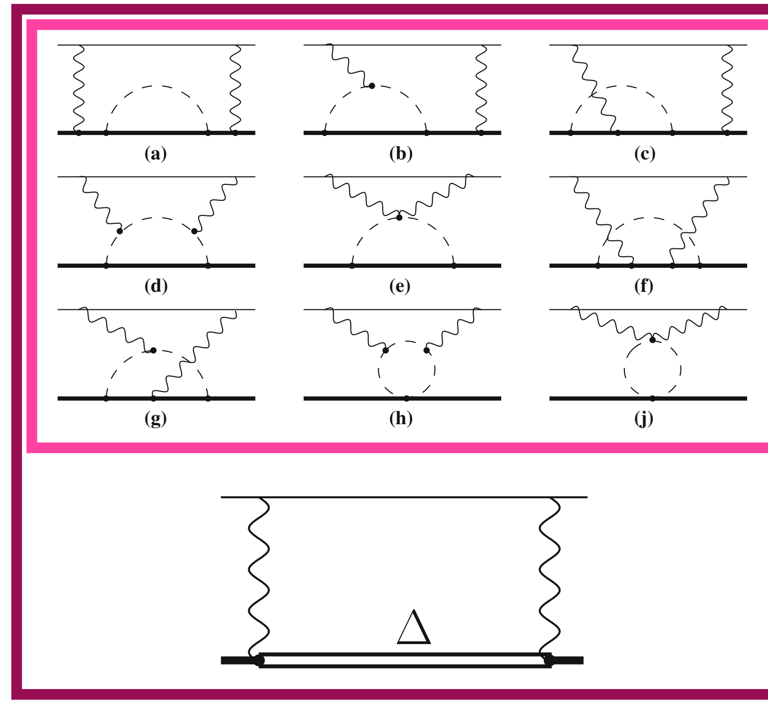

POLARIZABILITY EFFECT FROM BCHPT

- Low-Q region is very important!
- LO BChPT result is compatible with zero
  - Contributions from σ_{LT} and σ_{TT} are sizeable and largely cancel each other

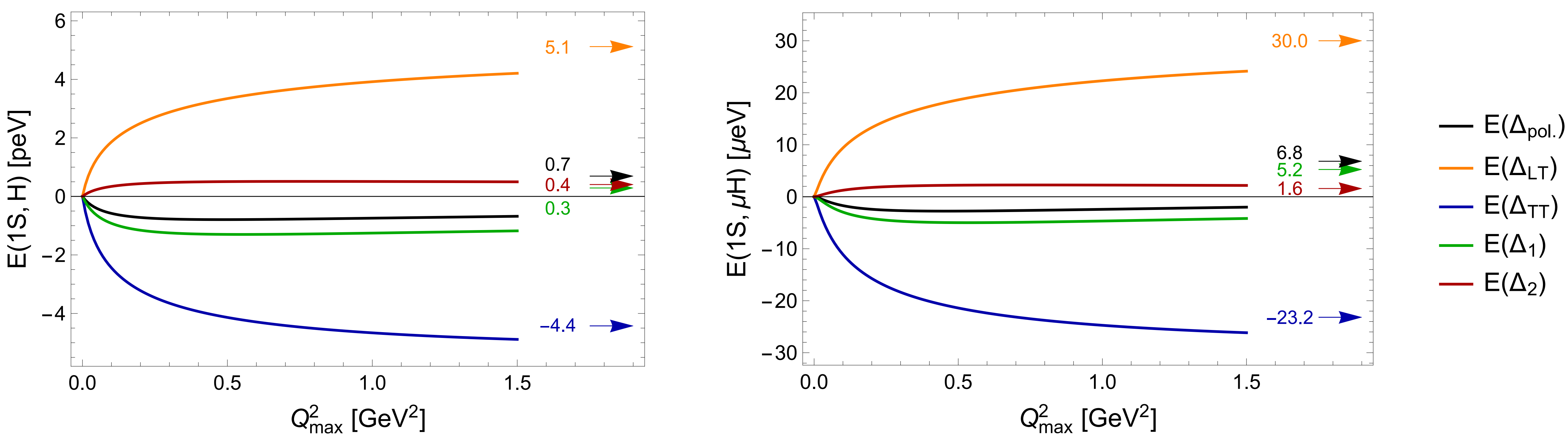

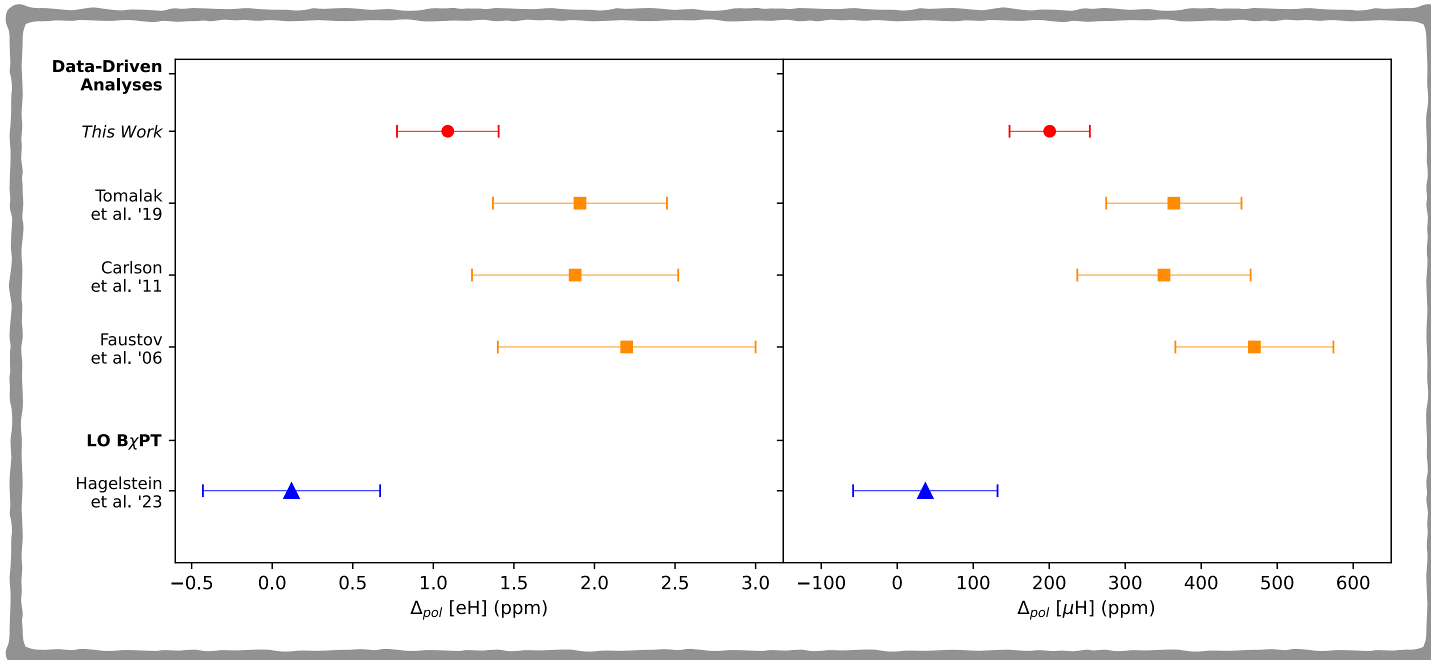

TTING IN μH

Experiment: HFS in μH, μHe$^+$, …

Testing the theory

- **discriminate between theory predictions for polarizability effect**
  - disentangle R_Z & polarizability effect by combining HFS in H & μH
- test HFS theory
  - combining HFS in H & μH with theory prediction for polarizability effect
- test nuclear theories

Determine fundamental constants

Zemach radius R_Z

Interpreting the exp.

extract E^{TPE}, $E^{\text{pol.}}$ or R_Z

Guiding the exp.

find narrow 1S HFS transitions with the help of full theory predictions: QED, weak, finite size, polarizability

Input for data-driven evaluations

form factors, structure functions, polarizabilities

Spectroscopy of ordinary atoms (H, He$^+$)

Electron and Compton Scattering

THEORY OF HYPERFINE SPLITTING

A. Antognini, FH, V. Pascalutsa, Ann. Rev. Nucl. Part. **72** (2022) 389-418

The hyperfine splitting of μH (theory update):

$$E_{1S\text{-hfs}} = \Big[\underbrace{182.443}_{E_\mathrm{F}} \underbrace{+1.350(7)}_{\mathrm{QED+weak}} \underbrace{+0.004}_{\mathrm{hVP}} \underbrace{-1.30653(17)\left(\frac{r_{\mathrm{Z}p}}{\mathrm{fm}}\right) + E_\mathrm{F}\left(1.01656(4)\,\Delta_\mathrm{recoil} + 1.00402\,\Delta_\mathrm{pol}\right)}_{2\gamma\ \text{incl. radiative corr.}}\Big]\,\mathrm{meV}$$

- 2γ + radiative corrections $\Longrightarrow$ differ for H vs. μH and 1S vs. 2S

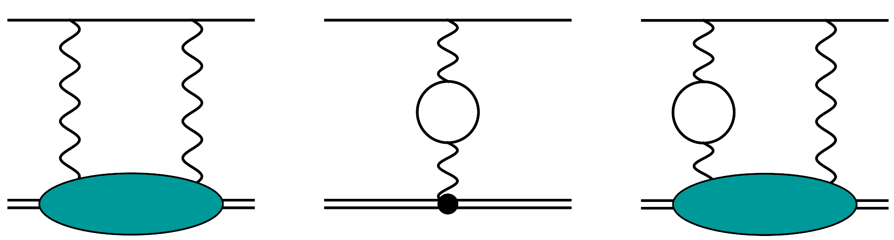

+ …

The hyperfine splitting of H (theory update):

$$E_{1S\text{-hfs}}(\mathrm{H}) = \Big[\underbrace{1\,418\,840.082(9)}_{E_\mathrm{F}} \underbrace{+1\,612.673(3)}_{\mathrm{QED+weak}} \underbrace{+0.274}_{\mu\mathrm{VP}} \underbrace{+0.077}_{\mathrm{hVP}}$$
$$\underbrace{-54.430(7)\left(\frac{r_{\mathrm{Z}p}}{\mathrm{fm}}\right) + E_\mathrm{F}\left(0.99807(13)\,\Delta_\mathrm{recoil} + 1.00002\,\Delta_\mathrm{pol}\right)}_{2\gamma\ \text{incl. radiative corr.}}\Big]\,\mathrm{kHz}$$

High-precision measurement of the "21cm line" in H:

$$\delta\left(E^{\mathrm{exp.}}_{1S-\mathrm{hfs}}(\mathrm{H})\right) = 10^{-12}$$

Hellwig et al., 1970

IMPACT OF H 1S HFS

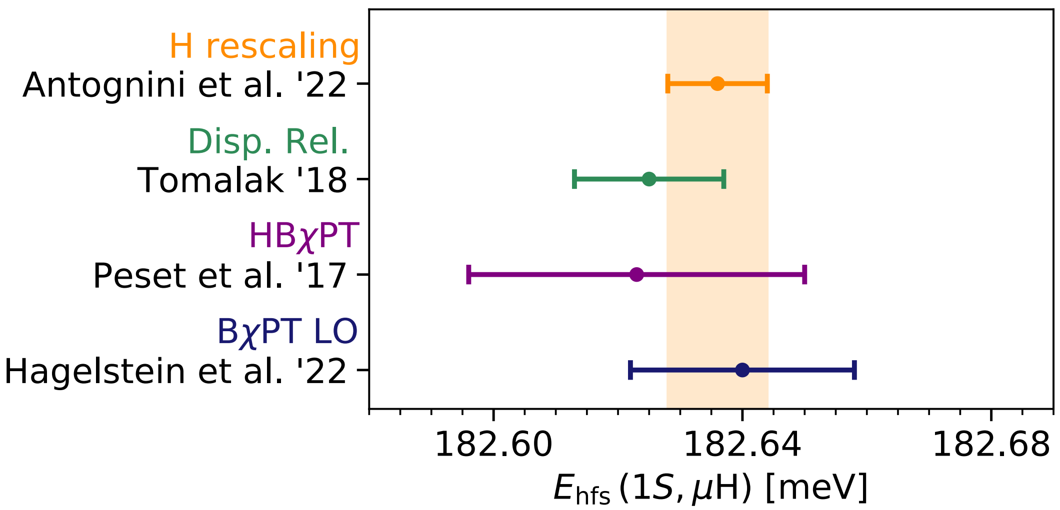

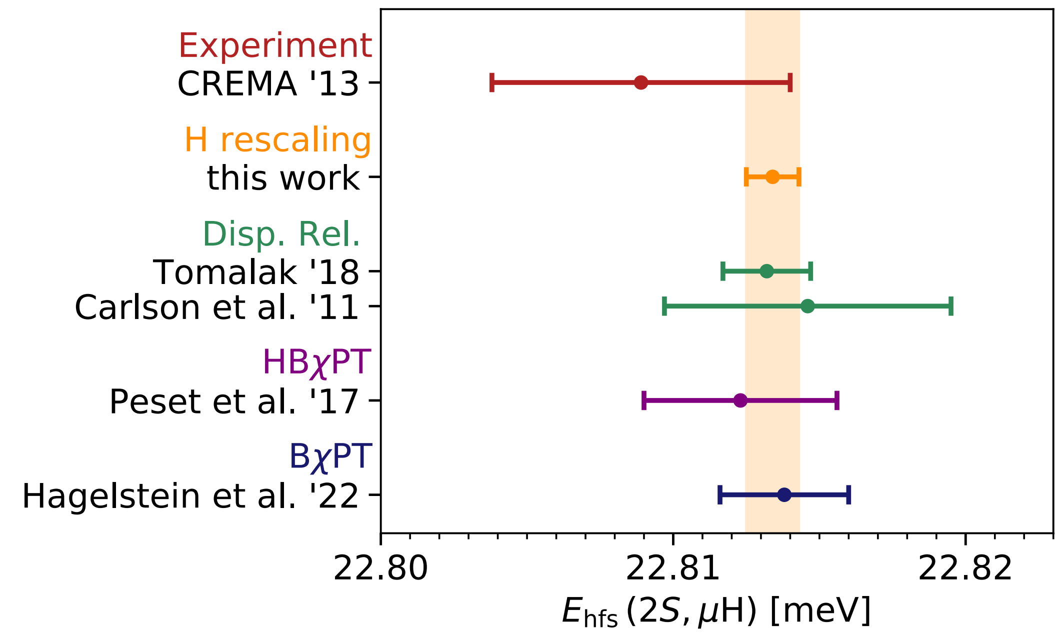

- Leverage radiative corrections $E^{\mathrm{Z+pol}}_{1S-\mathrm{hfs}}(\mathrm{H}) = E_{\mathrm{F}}(\mathrm{H})\Big[b_{1S}(\mathrm{H})\,\Delta_{\mathrm{Z}}(\mathrm{H}) + c_{1S}(\mathrm{H})\,\Delta_{\mathrm{pol}}(\mathrm{H})\Big] = -\,54.900(71)\,\mathrm{kHz}$ and assume the non-recoil $\mathcal{O}(\alpha^5)$ effects have simple scaling $\dfrac{\Delta_i(\mathrm{H})}{m_r(\mathrm{H})} = \dfrac{\Delta_i(\mu\mathrm{H})}{m_r(\mu\mathrm{H})}, \quad i = \mathrm{Z},\mathrm{pol}$

1. Prediction for μH HFS from empirical 1S HFS in H

$$E^{\mathrm{Z+pol}}_{nS-\mathrm{hfs}}(\mu\mathrm{H}) = \frac{E_{\mathrm{F}}(\mu\mathrm{H})\,m_r(\mu\mathrm{H})\,b_{nS}(\mu\mathrm{H})}{n^3 E_{\mathrm{F}}(\mathrm{H})\,m_r(\mathrm{H})\,b_{1S}(\mathrm{H})}E^{\mathrm{Z+pol}}_{1S-\mathrm{hfs}}(\mathrm{H}) - \frac{E_{\mathrm{F}}(\mu\mathrm{H})}{n^3}\,\Delta_{\mathrm{pol}}(\mu\mathrm{H})\quad \underbrace{\left[c_{1S}(\mathrm{H})\frac{b_{nS}(\mu\mathrm{H})}{b_{1S}(\mathrm{H})} - c_{nS}(\mu\mathrm{H})\right]}_{=\,-\,6\times10^{-5}\ \mathrm{for\ n=1}\quad =\,-\,5\times10^{-5}\ \mathrm{for\ n=2}}$$

2. Disentangle Zemach radius and polarizability contribution
3. Testing the theory

HYPERFINE SPLITTING IN μH

Theory: QED, ChPT, data-driven dispersion relations, ab-initio few-nucleon theories

Experiment: HFS in μH, μHe^+, …

Guiding the exp.

find narrow 1S HFS transitions with the help of full theory predictions: QED, weak, finite size, polarizability

Interpreting the exp.

extract E^{TPE}, $E^{\mathrm{pol.}}$ or R_Z

Input for data-driven evaluations

form factors, structure functions, polarizabilities

Electron and Compton Scattering

Testing the theory

- discriminate between theory predictions for polarizability effect
  - disentangle R_Z & polarizability effect by combining HFS in H & μH
- test HFS theory
  - combining HFS in H & μH with theory prediction for polarizability effect
- test nuclear theories

Spectroscopy of ordinary atoms (H, He^+)

Determine fundamental constants

Zemach radius R_Z

PROTON ZEMACH RADIUS

- BChPT polarizability prediction implies smaller Zemach radius (smaller, just like r_p)

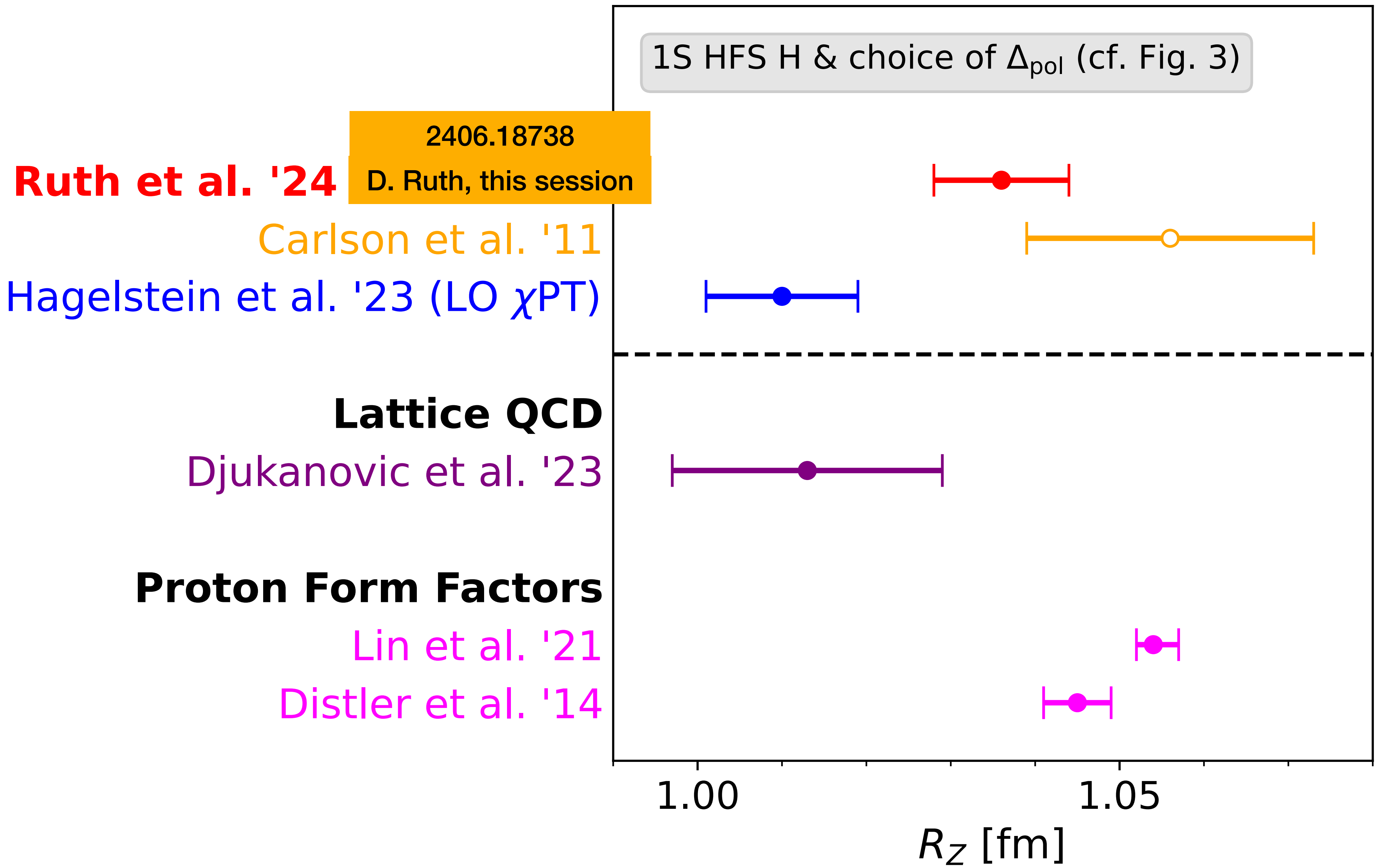

H.-W. Hammer, Wed.

CORRELATION OF PROTON RADII

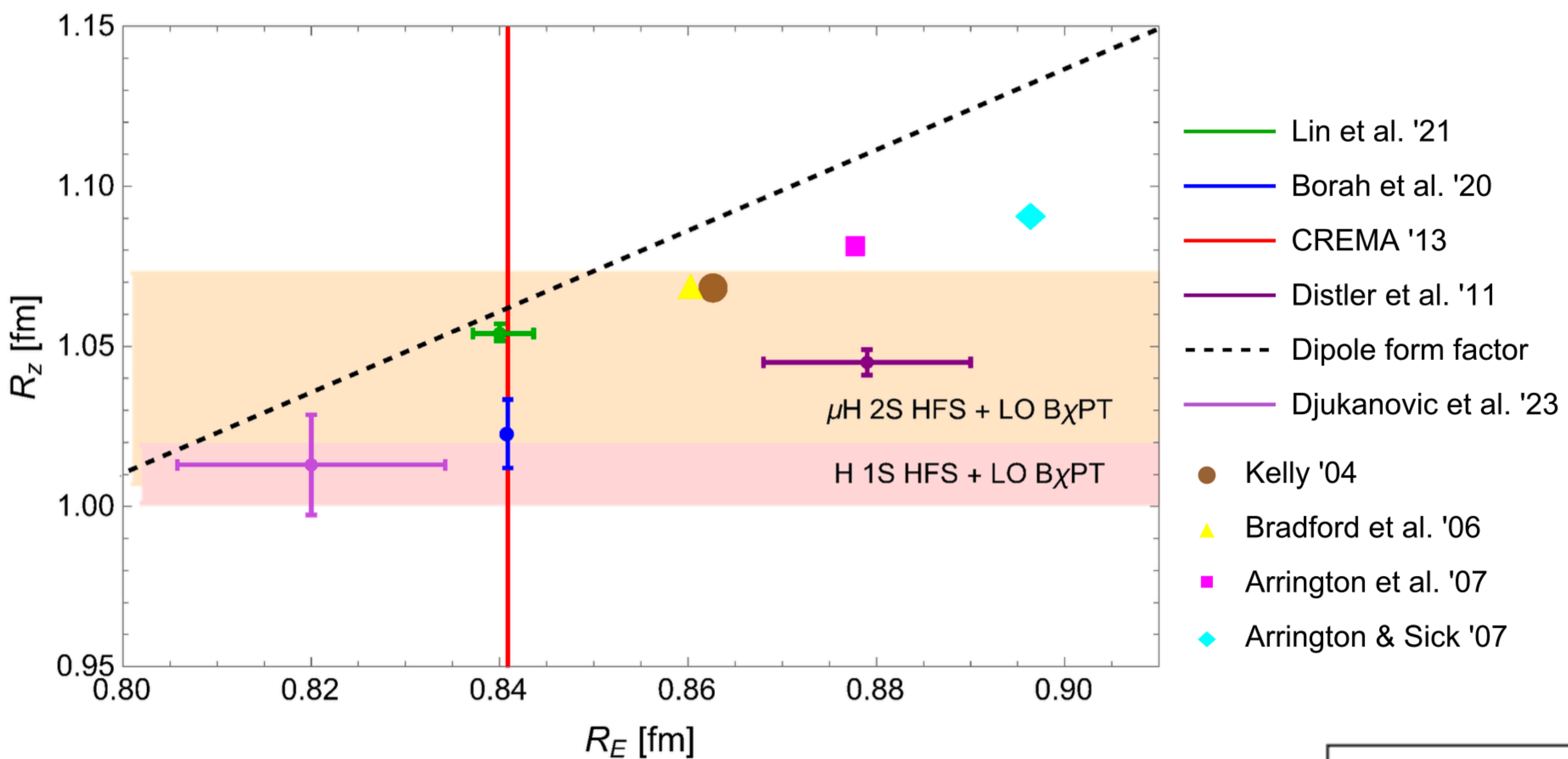

Zemach radius

$$R_Z \equiv -\frac{4}{\pi}\int_0^\infty \frac{\mathrm{d}Q}{Q^2}\left[\frac{G_E(Q^2)G_M(Q^2)}{1+\kappa}-1\right]$$

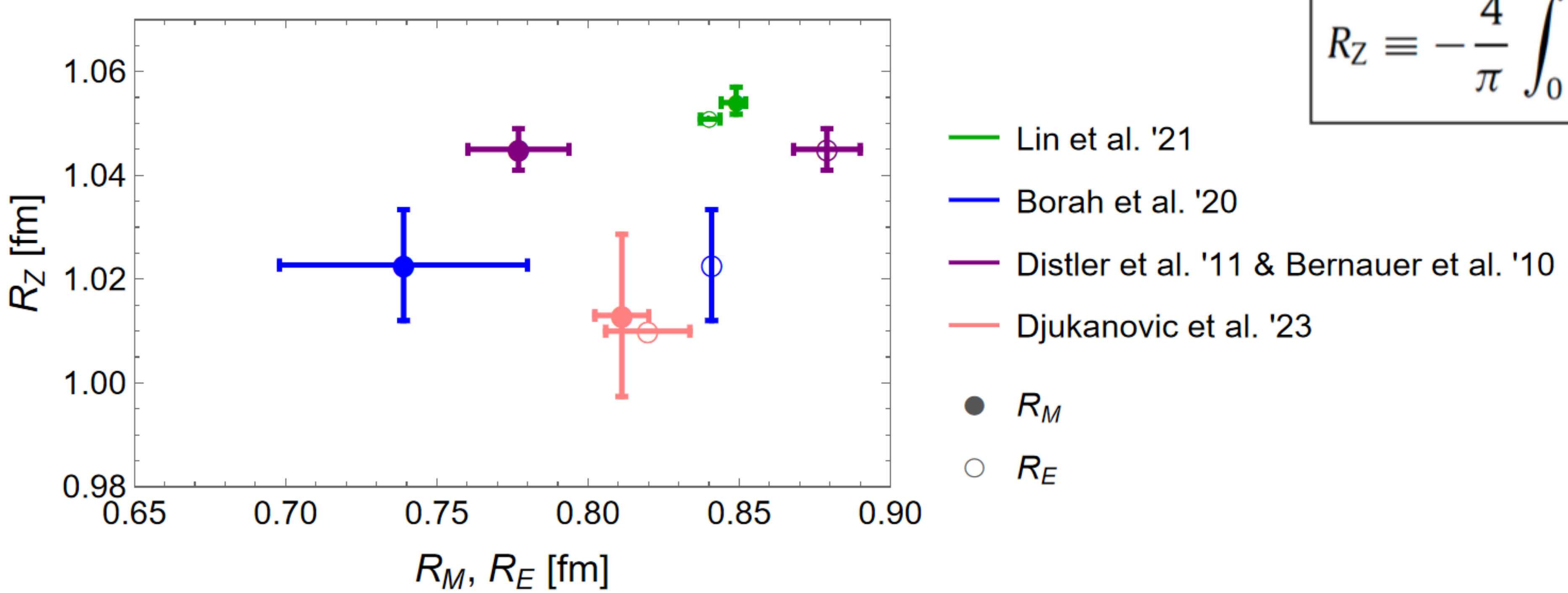

DEUTERON CHARGE RADIUS

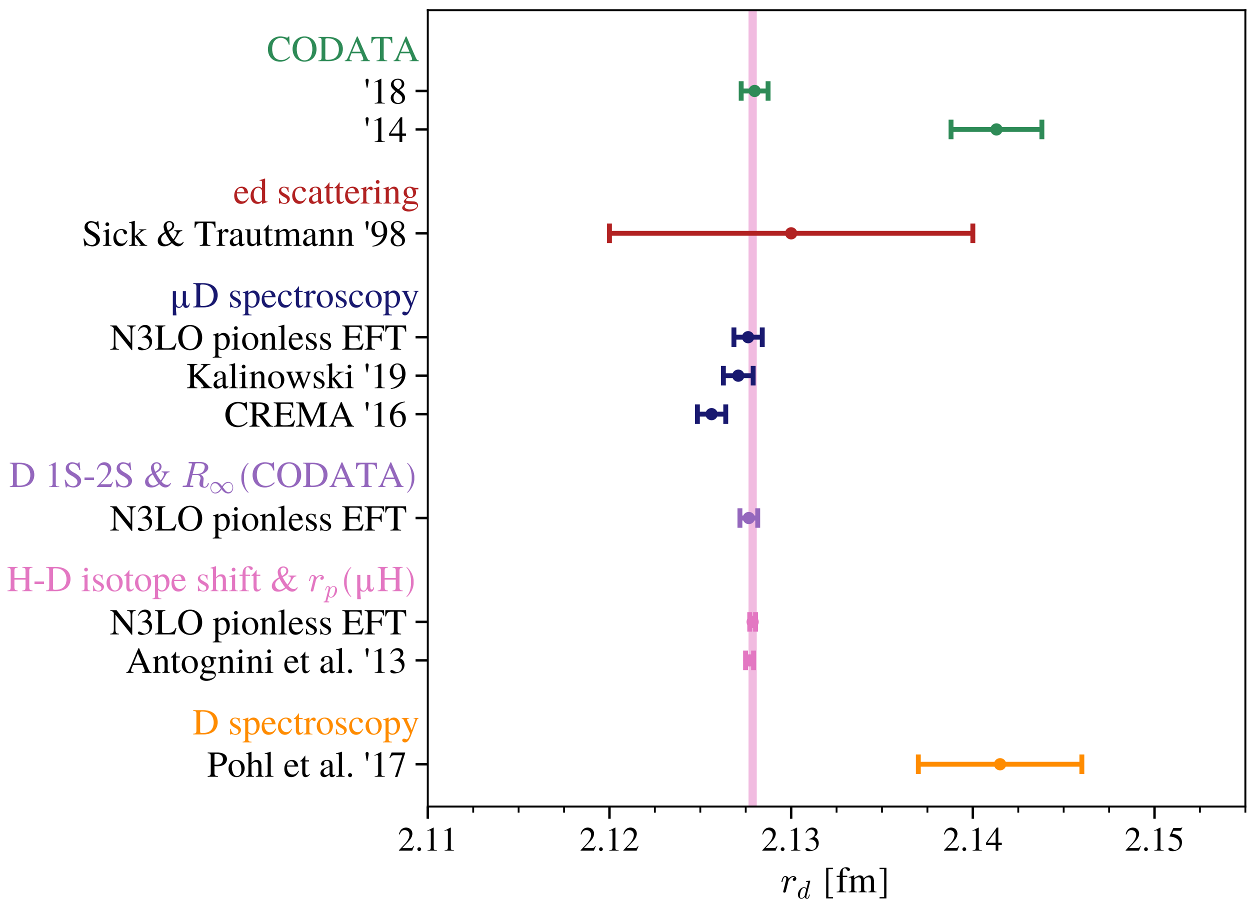

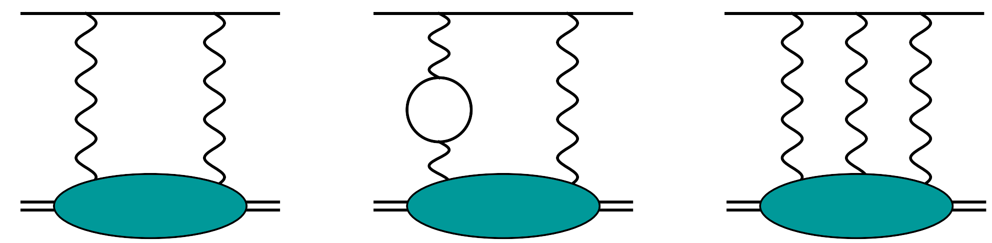

- Precise deuteron radius from H-D 1S-2S isotope shift and μH Lamb shift
- Higher-order contributions to μD Lamb shift are important:

$$E_{2P-2S}(\mu\mathrm{D}) = \left[228.77408(38) - 6.10801(28)\left(\frac{r_d}{\mathrm{fm}}\right)^2 - E_{2S}^{2\gamma} + 0.00219(92)\right]\ \mathrm{meV}$$

  - Coulomb (non-forward) distortion (starting $\alpha^6 \log \alpha$): $E_{2S}^{\mathrm{Coulomb}} = 0.2625(15)\ \mathrm{meV}$
  - 2γ incl. eVP and 3γ contributions starting α^6 [Kalinowski, Phys. Rev. A **99** (2019) 030501]

D FORM FACTOR IN PIONLESS EFT

V. Lensky, A. Hiller Blin, V. Pascalutsa, Phys. Rev. C **104** (2021) 054003

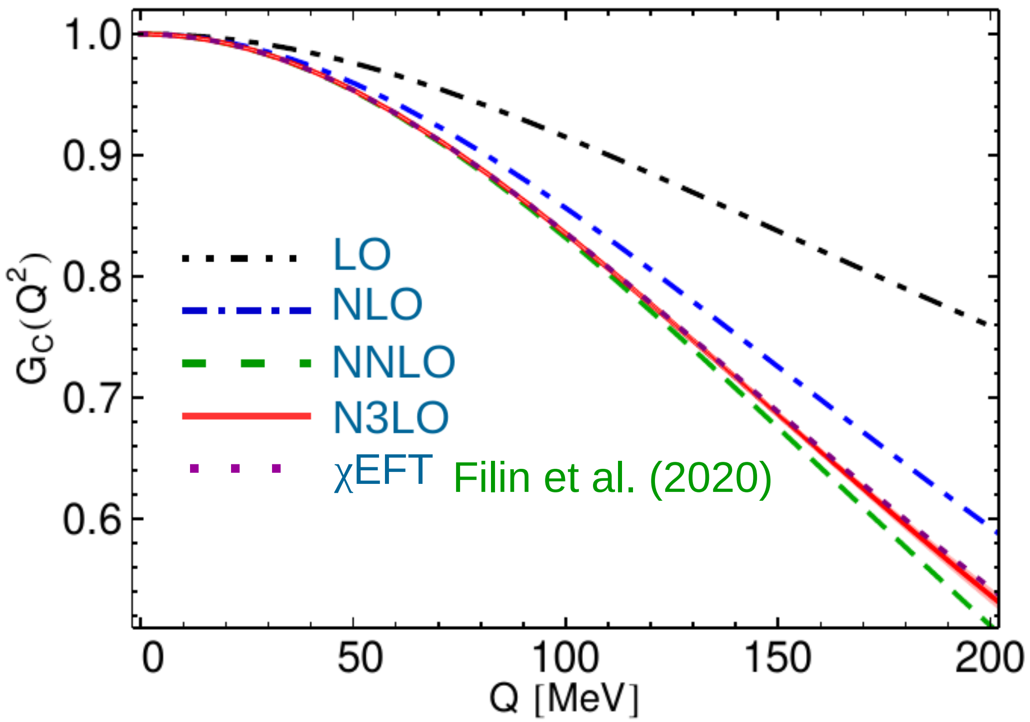

- Only one unknown low-energy constant l_1 of a longitudinal photon coupling to two nucleons
- Agreement of chiral EFT and pionless EFT

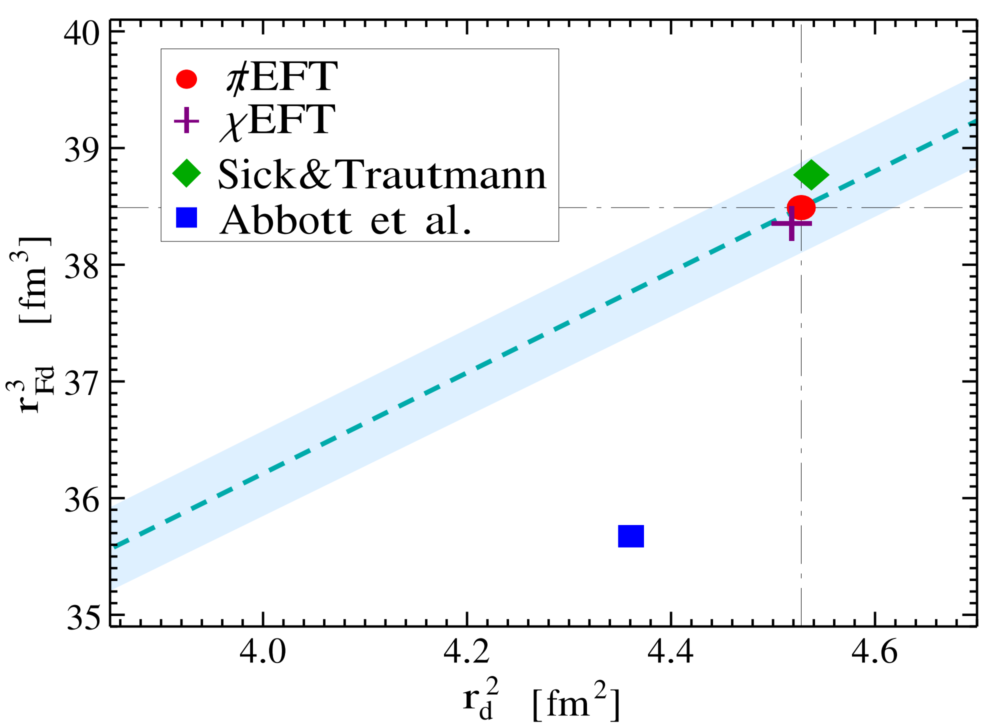

- Use r_d and r_{Fd} correlation to test low-Q properties of form factor parametrisations
- Abbott parametrisation gives different radii

2γ EFFECT IN μD LAMB SHIFT

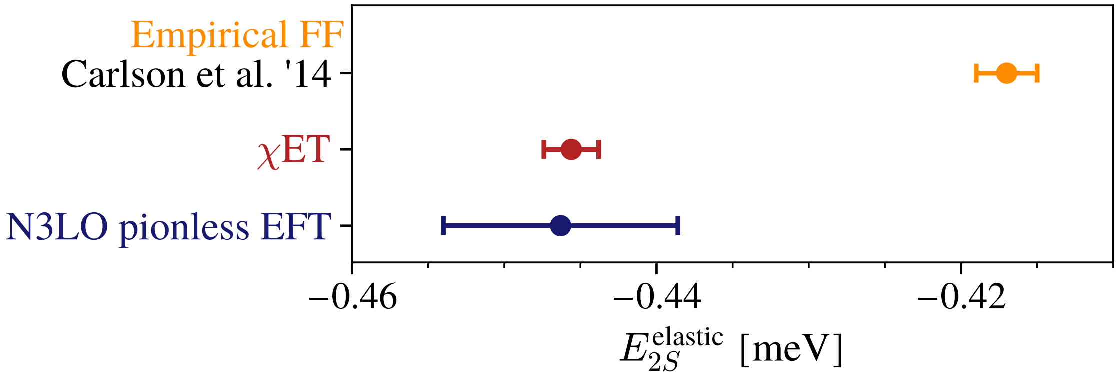

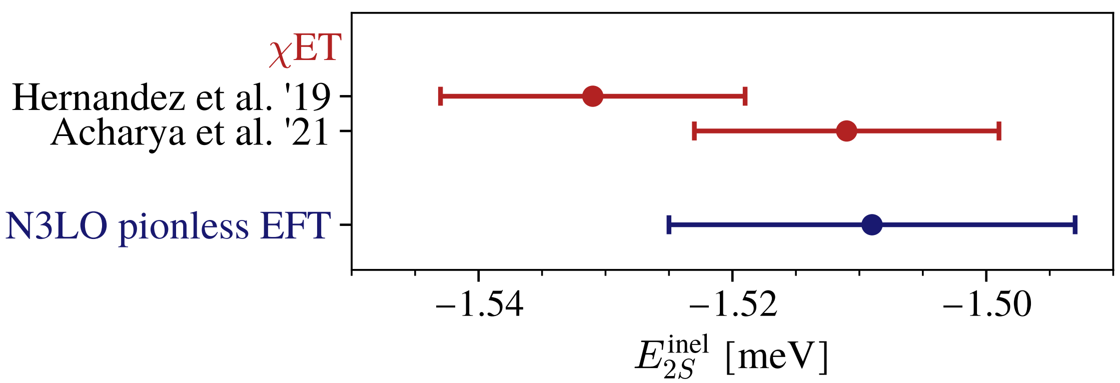

	$E_{2S}^{2\gamma}$ [meV]
Theory prediction	
Krauth et al. '16 [5]	$-1.7096(200)$
Kalinowski '19 [6, Eq. (6) + (19)]	$-1.740(21)$
$\not\pi$EFT (this work)	$-1.752(20)$
Empirical (μH + iso)	
Pohl et al. '16 [3]	$-1.7638(68)$
This work	$-1.7585(56)$

V. Lensky, FH, V. Pascalutsa, EPJ A 58 (2022) 11, 224 and PLB 835 (2022) 137500

- N3LO pionless EFT + higher-order single-nucleon effects:

$$E_{2S}^{\mathrm{elastic}} = -\,0.446(8)\,\mathrm{meV}$$
$$E_{2S}^{\mathrm{inel},L} = -\,1.509(16)\,\mathrm{meV}$$
$$E_{2S}^{\mathrm{inel},T} = -\,0.005\,\mathrm{meV}$$
$$E_{2S}^{\mathrm{hadr}} = -\,0.032(6)\,\mathrm{meV}$$
$$E_{2S}^{\mathrm{eVP}} = -\,0.027\,\mathrm{meV}$$

- Elastic 2γ several standard deviations larger
- Inelastic 2γ consistent with other results
- Agreement with precise empirical value for the 2γ effect extracted with $r_d\,(\mu\mathrm{H} + \mathrm{iso})$

PRECISION ATOMIC SPECTROSCOPY

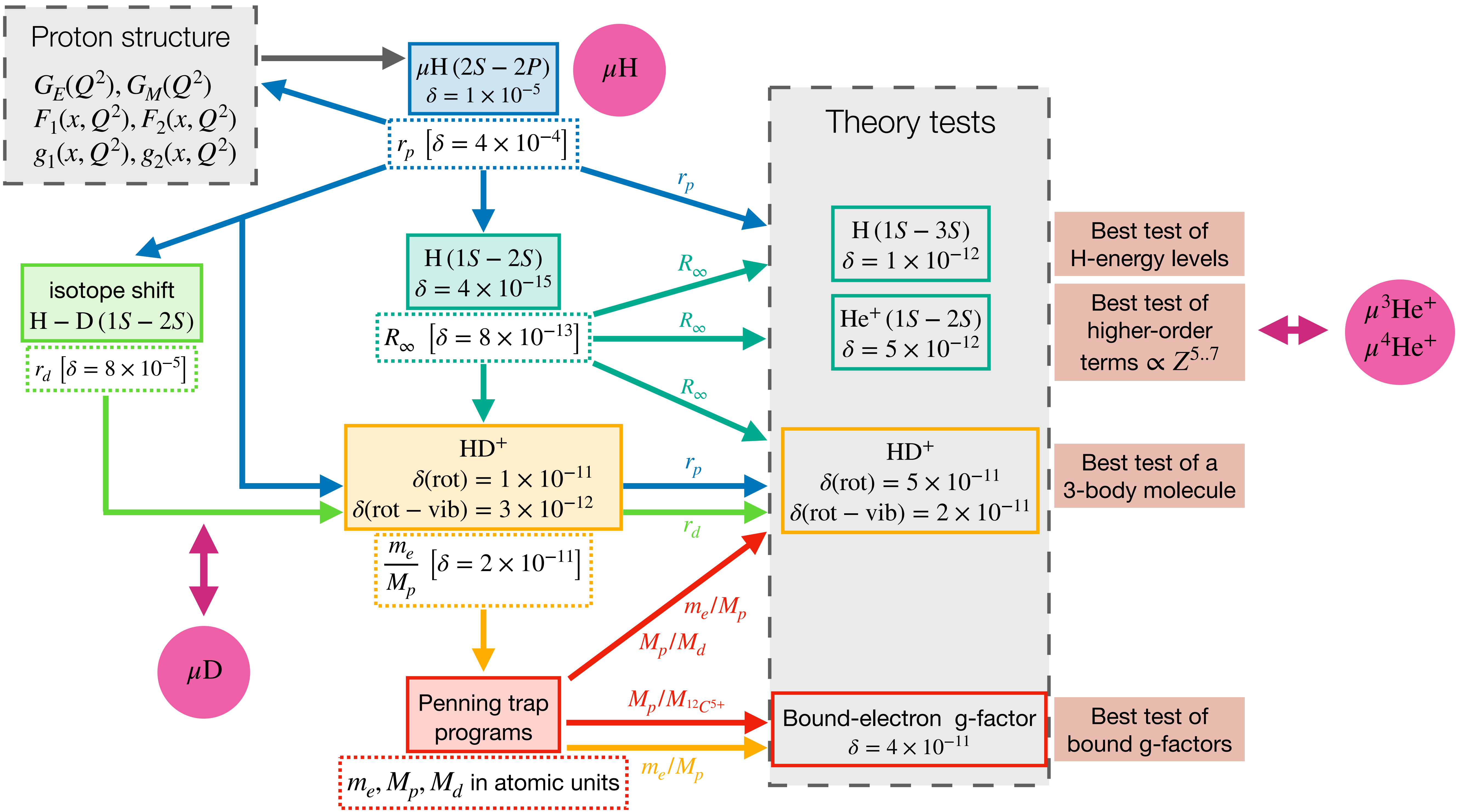

A. Antognini, FH, V. Pascalutsa, Ann. Rev. Nucl. Part. **72** (2022) 389

Thank you for your attention!